Fundamental aspects of sperm biology for ecologically and economically important bivalve species in Alabama: Cellular signaling, morphology, and density quantification

By

Zoe Grace Nichols

A thesis submitted to the Graduate Faculty of
Auburn University
in partial fulfillment of the
requirements for the Degree
of Master of Science

Auburn, Alabama
May 2, 2020

Keywords: cell signaling, channel blocker, freshwater mussel, microspectrophotometer, oyster, ultrastructure

Approved by

Ian A.E. Butts, Chair, Assistant Professor, School of Fisheries, Aquaculture, and Aquatic Sciences
James A. Stoeckel, Associate Professor, School of Fisheries, Aquaculture, and Aquatic Sciences
William C. Walton, Associate Professor, School of Fisheries, Aquaculture, and Aquatic Sciences
William Wayman, Center Director, U.S. Fish and Wildlife Service, Warm Springs Fish Technology Center

Abstract

The Eastern oyster, *Crassostrea virginica*, and freshwater mussels, *Ligumia subrostrata* and *Lampsilis straminea*, are significant keystone species in the Eastern United States. These bivalves both provide invaluable environmental enrichment services such as biofiltration and habitat stabilization. Oysters are economically valuable as they are one of the largest contributors to shellfish aquaculture production, while freshwater mussels are of interest due to their ecological contributions and intricate reproductive tactics and life histories. This thesis conducted studies on fundamental aspects of sperm biology for *C. virginica*, *L. subrostrata* and *L. straminea*.

Productive water along the coastline of Alabama supports many *C. virginica* farms, which usually rely on oyster seed provided by hatcheries. High fertilization success can increase oyster aquaculture production, and many aspects of sperm biology are linked to fertilization success, such as sperm motility. Thus, this thesis investigated the physiological aspects regulating sperm motility initiation. Different salinity, pH, and ion activation medias all impacted sperm activity parameters. These findings can be used to enhance fertilization success and assist with development of short-term storage and cryopreservation media.

Alabama is a global hotspot for freshwater mussel diversity. Unfortunately, they are in steep decline. Conservation efforts are focusing on propagation techniques to save these imperiled organisms. However, there is limited information regarding seasonal sperm production and morphology, as well as efficient techniques to quantify sperm production regarding freshwater mussels. Thus, this thesis examined sperm densities and morphology across the

spawning season of *L. subrostrata* and *L. straminea*. Both species displayed an increase and subsequent decrease in sperm concentration over the sampling period as well as an increase in sperm head morphology over time. Tools were also developed using microspectrometery and regressions to accurately estimate sperm concentrations. The seasonal spawning data and microspectrometery techniques can contribute towards propagation efforts and cryopreservation techniques of freshwater mussels.

Acknowledgments

First, I express my sincere gratitude to my research advisor, Dr. Ian A. E. Butts, for giving me the opportunity to conduct research and providing invaluable guidance and support throughout my graduate studies at Auburn University. Dr. Butts provided me with continuous positive feedback on my research projects, posters, presentations, and writing this thesis. I also thank him for the valuable statistical support on my research.

I thank the other members of my graduate committee, Dr. James Stoeckel, Dr. William Walton, and Dr. William Wayman for the beneficial insights they provided towards completion of this thesis. Additionally, I would like to thank Dr. S. M. Hadi Alavi for constant assistance throughout the Eastern oyster study and for meticulously reviewing my oyster thesis work.

I give my upmost gratitude to the Auburn University Shellfish Laboratory graduate students, Victoria Pruente, Sarah Henesey, and MC Eastburn, and staff, Caitlin Robitaille and Sarah Spellman, for everything they do to keep the lab running smoothly and for caring for the oysters that were used in this thesis. Thank you, Glen Chaplin for taking me out on the boat to collect my research oysters. I give a special thanks to Scott Rikard for providing his assistance throughout the study and helping with the shipping of oysters. Additionally, I am extremely appreciative of Kelsey Bisker and Madison McGough for warmly opening their home to me and for their extremely comfortable beanbag throughout the duration of my stay on Dauphin Island.

A special thanks to the Auburn University Crustacean & Molluscan Ecology Laboratory for providing the ponds and freshwater mussels to make this study possible. I am very appreciative to Kaelyn Fogelman, Rebecca Tucker Gibson, Amanda Strozier, Austin Haney, and Ryan Fluharty who all tremendously helped collect freshwater mussels with me at South Auburn.

Thank you, Dr. Michael Miller for your guidance throughout the numerous steps of SEM and TEM and trusting me with the microtome. Additionally, I express my deepest appreciation to Vaishnavi Dalal for her countless hours spent in the lab. Our staining results could not have been done without your meticulous work ethic.

Finally, I would like to thank my parents, Katherine and Charles Nichols, for their love and support. They provided me with continuous encouragement throughout the process of researching and writing this thesis, and this accomplishment would not have been possible without them.

Table of Contents

Chapter 2: Quantifying sperm concentration and morphology for two species of unionid mussels

List of Figures

List of Tables

Chapter 1

Physiological mechanisms regulating sperm motility initiation in Eastern oyster, *Crassostrea virginica*

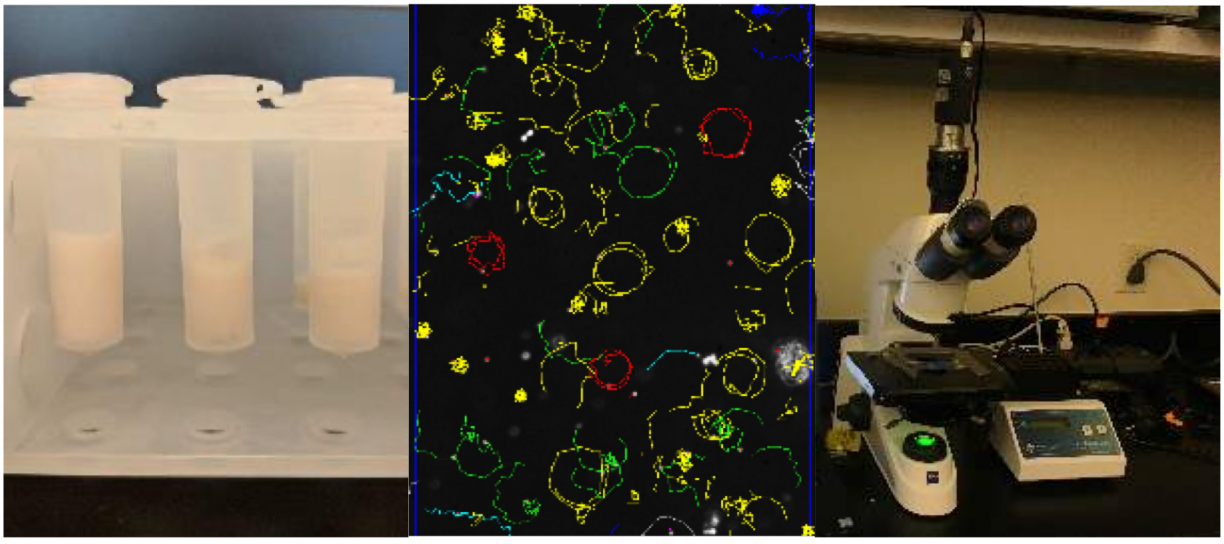

Nichols, Z.G., Rikard, S., Alavi, S.M.H., Walton, W.C., & Butts, I.A.E. Physiological mechanisms regulating sperm motility initiation in Eastern oyster, *Crassostrea virginica*. To be submitted to *PLOS ONE* in April 2020

Abstract

Oyster aquaculture is expanding in the United States, where production has increased from $78 million to $192 million between 2008 to 2016. Many oyster farms rely on oyster seed produced at hatcheries that induce broodstock to spawn. Hatchery success can often be dependent on gamete quality. In order to improve hatchery production, a better understanding of oyster gamete biology is needed. Eastern oyster, *Crassostrea virginica,* males and females release sperm and oocytes into the water column to be fertilized. Upon release, non-motile sperm is exposed to external environment factors which initiate sperm motility. Sperm motility performance is a key determinant for fertilization success. Thus, providing optimal environmental conditions will maximize sperm activity and fertilization success. The objectives of this work were to determine the physiological mechanisms regulating sperm motility initiation in *C. virginica*. Sperm swimming kinematics were evaluated by computer assisted sperm analysis, and curvilinear velocity (VCL) and percentage of motility were measured. Sperm activation was measured in artificial sea water (ASW) across pH gradient from pH 6.5 to 10.5 and a range of salinities from 4 to 32 practical salinity units (PSU). Artificial sea water was modified with 0.5 to 3.5 mM EGTA to find the concentration of EGTA needed to inhibit sperm motility. Na^+, K^+, Mg^{2+}, and Ca^{2+} free ASW and their respective channel blockers were used to elucidate ionic signaling involved in sperm motility initiation. Results show that sperm motility was highest from pH 6.5 to 7.5 and salinity from 12 to 24 PSU. Compared to baseline ASW, sperm motility was lower in Na^+, K^+, Ca^{2+}, and Mg^{2+} free ASW. Moreover, sperm motility initiation was suppressed in the presence of K^+ and Ca^{2+} channel blockers. These results show that pH and environmental salinity affects sperm motility initiation and indicate that sperm motility initiation is Ca^{2+}-dependent and

requires K^+ exchange through the plasma membrane. Our study provides insights into physiological mechanisms of sperm motility signaling in bivalves and provides valuable information to improve fertility in hatcheries and optimize short-term storage and sperm cryopreservation protocols.

1.1. Introduction

For many aquatic species possessing external fertilization strategies, fully mature sperm is non-motile in the gonad and reproductive tracts (Cosson et al. 2008; Demoy-Schneider et al. 2014). Once sperm is released into the aquatic environment, initiation of sperm motility (flagellar beating) is triggered by osmotic or ionic differences in the aquatic environment compared to the seminal plasma (Morisawa and Suzuki 1980; Alavi and Cosson 2005, 2006; Dzyuba and Cosson 2014). Sperm subsequently has a limited period of motility to reach an oocyte while it is still viable (Billard 1983; Rurangwa et al. 2004; Song et al. 2009). Thus, sperm quality (ability to successfully fertilize an oocyte and produce a viable embryo) is strongly affected by factors affecting motility (Bobe and Labbé 2010).

Sperm motility has been linked to male reproductive potential, where high fertilization rates are often required for reproductive success (Billard et al. 1995; Levitan 1995). It is worth noting that sperm quality can vary among wild and cultivated broodstock (Butts et al. 2010, 2011) and while male-to-male variability in gamete quality is documented, it is often poorly understood (Bobe and Labbé 2010). The most critical indicators of sperm quality are motility kinetics (i.e. percentage of motile sperm following release into the aquatic environment) and velocity (Billard 1978; Stoss 1983; Lahnsteiner et al. 1996). These estimators can be measured using computer-assisted sperm analysis (CASA) software, which uses video frames to track sperm head trajectories (Kime et al. 1996; Rurangwa et al. 2001; Cosson 2008).

Investigating physiological mechanisms maintaining sperm in the quiescent state in the reproductive organ and regulating sperm motility initiation after discharge into the aquatic environment can provide us with valuable information to develop and refine methods for

artificial reproduction, methods for short- or long-term preservation of sperm, and protocols for evaluating inter-individual differences in fertilizing ability of sperm (Alavi et al. 2008, 2019).

A common suite of osmotic or ionic signals regulate sperm motility initiation in many aquatic species (Cosson 2015; Alavi et al. 2019), including bivalves. For instance, external pH which is one of the key triggers for sperm motility initiation in the sea urchin (*Strongylocentrotus purpuratus*) and in marine bivalves, also affects sperm velocity (Christen et al. 1983; Alavi et al. 2014; Boulais et al. 2018). It has been shown that low environmental pH inhibits reproduction of the Eastern oyster (*Crassostrea virginica*) (Prytherch 1928), sperm motility initiation in the Pacific oyster (*C. gigas*), Manila clam (*Ruditapes philippinarum*), and Japanese scallop (*Patinopecten yessoensis*) (Boulais et al. 2018), and ATPase activity in the sea urchin (Christen et al. 1983).

In addition to pH, sperm motility initiation in marine bivalves partly depends on the salinity of the aquatic environment. Salinity directly effects reproduction of aquatic species, where low salinities reduced fertilization and larval development in the Pacific oyster (Kinnby et al. 2015) and sperm motility and fertilization success of the sea urchin (Dinnel et al. 1987). Ions including calcium (Ca^{2+}), potassium (K^{+}), magnesium (Mg^{2+}), and sodium (Na^{+}) also play critical roles in signal transductions that regulate sperm motility initiation (Boulais et al. 2018, 2019). These ions are also found in the seminal plasma (Alavi and Cosson 2006; Alavi et al. 2019; Boulais et al. 2019). Overall, environmental osmolality, pH and ions are responsible for both motility initiation as well as maintaining sperm in the quiescent state (Morisawa et al. 1983b, 1983c, 1983a; Morisawa 1985).

To elucidate physiological mechanisms regulating sperm motility initiation, the role of osmolality, pH, and ions can be understood by decreasing or increasing their values compared to

the values in the seminal plasma, or by completely removing the ion from the sperm activating solution, or by application of a proper channel blocker which inhibits ionic fluxes across the sperm membrane. A voltage-dependent K^+ channel blocker, 4-aminopyridine (4-AP), is known to inhibit sperm motility initiation in bivalves (Alavi et al. 2014) similar to that of fish (Krasznai et al. 1995). Additionally, the ATP-sensitive K^+ channel blocker, glybenclamide, has been used to investigate the inhibiting effects on sperm activity (Zilli et al. 2008). These suggest that K^+ efflux though a K^+ channel is required for sperm motility initiation (Krasznai et al. 1995; Alavi et al. 2014).

Similar to most freshwater and seawater fish species (Morisawa 2008; Alavi et al. 2019) sperm motility initiation in bivalves requires Ca^{2+}, as the percentage of motile sperm decreases after diluting sperm with seawater that contains ethylene glycol-bis(β-aminoethyl ether)-N,N,N′,N′-tetraacetic acid (EGTA), a chelator of Ca^{2+} ions (Alavi et al. 2014). Moreover, sperm motility initiation was also inhibited in the presence of mibefradil (a T-type Ca^{2+} channel blocker), verapamil (a L-type voltage-dependent Ca^{2+} channel blocker), and nifedipine (a general L-type and a T-type Ca^{2+} channel blocker) (Lievano et al. 1996; Krasznai et al. 1995, 2000; Mocanu et al. 1999; Butts et al. 2013; Alavi et al. 2014).

Initiation of sperm motility in bivalves was also reduced in Na^+-free seawater, and a Na^+/Ca^{2+} exchanger is involved (Faure et al. 1994; Alavi et al. 2014; Boulais et al. 2018). It is also reported that a Na^+/H^+ exchanger is involved in the regulation of intracellular pH of bivalve sperm (Boulais et al. 2018). Amiloride, a channel blocker that prevents Na^+/H^+ exchange, inhibits motility in fish (Detweiler and Thomas 1998; Vílchez et al. 2016). The Mg^{2+} ion is found in seminal plasma and is a common ion found naturally in seawater; thus, the effect of Mg^{2+} on

sperm motility of fish and bivalves is often investigated (Alavi et al. 2004; Le et al. 2011; Le and Pham 2017; Boulais et al. 2018).

The Eastern oyster is native to benthic habitat along the Atlantic coast of America from Canada to the Gulf of Mexico, the Caribbean, and the coast of South America (Kennedy 1996). This bivalve mollusk is a keystone species providing many ecological services and economic value to the United States (Ozbay et al. 2017). Since the mid 1800s, wild oyster populations in the Mid-Atlantic and Gulf Coast of the United States have declined due to overharvesting, habitat degradation, and poor water quality (Kennedy 1996). Restoration efforts are hindered by increasing land development and fatal diseases which devastate oyster populations and recruitment (Ewart and Ford 1993; Ford and Tripp 1996; Ozbay et al. 2017).

Aquaculture has expanded across the Eastern United States to meet market demands and fill the low yield of the collapsed fishery. Oyster production, including the Eastern oyster, was valued at $192 million in 2016 (NMFS 2018). However, widespread diseases and the availability and quality of oyster seed to farms are bottlenecks for oyster production (Naylor et al. 2000; Jackson et al. 2001). Historically, the oyster industry relied on collecting wild spat from the environment, but anthropogenic impacts such as the Deepwater Horizon oil spill in 2010 have negatively affected reproductive success (Yang et al. 2012; Vignier et al. 2017). Thus, contemporary research is now directed towards artificial spawning of broodstock to supply oyster seed to farms. However, our knowledge about sperm biology in this species is very limited.

Although tolerant of a wide range of salinities (Galtsoff 1964; Wallace 1966), the Eastern oyster typically inhabits estuaries and bays with salinities less than full-strength seawater (30-33 PSU). The optimal salinity for the Eastern oyster is 14-28 PSU (Chanley 1958; Galtsoff 1964).

This raises the question as to whether sperm motility initiation cues will differ in type and intensity compared to bivalves that prefer different salinity ranges. Moreover, an understanding of the factors inhibiting and triggering the initiation of sperm motility is needed to support the current development of aquaculture that is oriented towards controlled crosses, selective breeding, and gamete cryobanking (Piferrer et al. 2009).

In the present study, our main goal was to investigate the physiological mechanisms involved in regulation of sperm motility initiation in the Eastern oyster. The objectives were to study the contribution of salinity, pH, and ions in sperm motility signaling. In this context, we evaluated the percentage of motile sperm and curvilinear velocity (VCL) in a series of pH activating solutions ranging from 5.0 to 11.0 and in salinity solutions ranging from 4 to 32 PSU. Then, we made Ca^{2+}-, K^{+}-, Mg^{2+}-, and Na^{+}-free artificial seawater (ASW) to examine the requirements of these ions for sperm motility initiation. Thereafter, we applied EGTA and various channel blockers for Ca^{2+}, K^{+}, and Na^{+} ions to better understand ionic signaling upon motility initiation.

The results of this study provide insights into the cellular processes behind motility initiation of the Eastern oyster which might be used to improve artificial fertilization in hatcheries and to assist in sperm storage protocol development and gene banking. In addition to this, our study provides biologists with valuable information to better elucidate environmental physiology of reproduction in bivalves by comparison of the Eastern oyster that reproduce in lower salinity with those of other species that reproduce in full-strength seawater with salinity of ~32 PSU.

1.2 Materials and Methods

1.2.1 Animal collection and husbandry

Oysters were collected in batches from floating cages and longline systems at the Auburn University Shellfish Laboratory research oyster farm site in Grand Bay, AL (30°22’34.8” N 88°18’52.8” W). Oysters were transported to the Auburn University Shellfish Laboratory (AUSL) in Dauphin Island, Alabama (30°14’51.9” N, 88°4’46.9” W) or the Auburn University Reproductive Physiology Laboratory in the E.W. Shell Fisheries Center, Auburn, Alabama (32° 40' 1.5" N, 85° 29' 22.1" W). At AUSL, the oysters were held in a flow-through system at 19°C and 10 PSU. All oysters were oriented cup side down in plastic crates (18” L x 12” W x 4” H). The incoming seawater flowed through a 50-micron pleated filter cartridge (Big Blue, Pentair Aquatic Eco-Systems, Inc., Apopka, FL) and was chilled with a 1/3 HP Trimline Delta Star Water Chiller.

At the Reproductive Physiology Laboratory, oysters were acclimated and held in a recirculation aquaculture system (RAS). The RAS system consisted of two 210-gal polyethylene round open top tanks (121.92 cm diameter × 81.28 cm height) (DC-501210, Dura-Cast Products, Inc., Lake Wales, FL). Seawater was made by mixing Crystal Sea Marinemix (Marine Enterprises International, LLC., Baltimore, MD) into water filtered through a reverse osmosis system (Barracuda Glacial 100 GPD RO/DI, AquaFX, Winter Park, Florida) to reach a salinity of 10 PSU to match the environmental salinity where oysters were collected. An additional 210-gal tank was filled with aerated reverse osmosis water which was used to manually replace

evaporated water in the RAS holding the oysters to maintain a constant water volume and salinity.

Water flowed from the bottom of the tanks into two connected sumps (105.41 cm length × 37.47 cm width × 50.8 cm height), which supplied the pump (1/2 HP Performance Pro Cascade, Performance Pro Pumps, Hillsboro, OR). Water flowed from the pump to a bubble bead filter (Aquaculture Systems Technology, Baton Rouge, LA), UV sterilizer (E120S, Emperor Smart UV High-Output Sterilizer, Pentair Aquatic Eco-Systems, Inc., Apopka, FL), and then to a 1 HP Delta Star In-line Water Chiller (DS-9, Aqua Logic, Inc., San Diego, CA), before re-entering the tanks. Water temperature was maintained at 19°C. Oysters were suspended via 3 cylindrical baskets (14" diameter × 14.5" height) per tank. Each day, the oysters were fed ~40 mL of Shellfish Diet 1800 (Reed Mariculture Inc., Campbell, CA).

1.2.2 Sperm collection

Oysters were opened with a shucking knife, cup-side down, at the hinge. The adductor muscle was carefully cut to remove the top shell. Once open, the oysters were assessed to determine if they were male or female by taking a small sample from the gonad and identifying sperm or eggs under a microscope. Only one male was processed at a time. Morphometrics such as length (± 0.01 mm), width (± 0.01 mm), height (± 0.01 mm), and weight (± 0.01 g) were recorded. The male was then thoroughly rinsed with distilled water to flush away any excess saltwater. The mantle tissue around the gonad area was dried with paper towels before testicular fluid (containing sperm and seminal plasma; hereafter "semen") was extracted. Approximately 20 µL of semen was collected from each male and stored in a 1 mL Eppendorf tube. Samples

were then placed into a chilling block (EchoTherm™ IC50, Torrey Pines Scientific, Inc., Carlsbad, CA, USA) set to 19°C. An aliquot of each sample was examined on a glass slide to ensure the sperm was not moving prior to the start of each experiment. If the sperm sample was contaminated with seawater during collection, motile sperm was observed, and the sperm sample and male were not used in the study.

1.2.3 Sperm motility assessment and testicular fluid characteristics

Computer assisted sperm analyses

Sperm activating solutions (500 to 1000 µL) were pipetted into 1 mL Eppendorf tubes, which were placed into the chilling block set to 19°C for the duration of the experiment. To activate sperm motility, 0.20 to 1.0 µL of semen was pipetted into various sperm activating solutions (see Section 1.2.4. to 1.2.6.). The tube was then inverted several times to mix thoroughly. At 1 min post-activation and thereafter, sperm motility was observed with a light microscope (AX10 Lab.A1, Carl Zeiss Meditec Inc., CA, USA) at 20× magnification. The suspension of semen with activating solution (5 µL) was then pipetted into a 20 µm deep 2X-CEL chamber (Hamilton Thorne Biosciences, Beverly, MA, USA), and videos were recorded from 1 to 180 min (see Section 1.2.4. to 1.2.6.).

Sperm activity was recorded and analyzed using a CASA (CEROS II, Hamilton Thorne Biosciences, Beverly, MA, USA) system. Percentage of motile sperm and VCL were analyzed for each observation. CASA sperm detection parameters were optimized after manual adjustments. Camera settings were as follows: images were taken at 60 frames per second,

exposure was set at 4 milliseconds, and camera gain at 300. For cell detection, cells were tracked with sizes between 3 to 11 μm, minimum cell brightness was set at 57, and the photometer range of the illumination fields were between 55 and 65. Each recorded video frame was checked manually for tracking accuracy. Sperm tracks were removed from analyses if the software incorrectly combined crossing tracks of multiple sperm, split the track of a single sperm, or if a cell exited the observation window before being adequately tracked (Butts et al. 2013).

Osmolality and pH of the testicular fluid

Male oysters (n = 5) were processed and semen was collected to measure osmolality and pH of the testicular fluid on 5 June 2019 (Table 1.1). To determine osmolality, 10 μL was pipetted onto the Wescor Vapro® Model 5600 Vapor Pressure Osmometer (Wescor, Inc, Logan, Utah, USA). Osmolality readings were repeated three times for each male, and the average was taken. The pH of testicular fluid and activation solutions were recorded with a benchtop pH meter (Orion Star™ A111 Benchtop pH Meter, Thermo Fischer Scientific, Madison, WI, USA) and an electrode (Orion™ PerpHecT™ ROSS™ Combination pH Micro Electrode, Thermo Fischer Scientific, Madison, WI, USA). The probe was rinsed in deionized water and dried between readings.

Sperm cell density

Sperm cell density (cells/mL) was calculated for each male (Table 1.2). To do this, 0.2 to 1 μL of semen was added into 999.8 to 999.0 μL of seawater with a salinity of 32 PSU to act as

an immobilizing media, determined based on observations explained in section 1.2.4. The samples were homogenized for ~10 s, then 10 μL was pipetted onto the Neubauer hemocytometer. Sperm randomly settled onto a 5 × 5 grid (1 mm^2), where sperm inside of five squares (0.2 mm^2) (top left, top right, bottom right, bottom left, and center) were counted. To get the average cell density of the diluted sperm in the 5 × 5 grid, the five squares were averaged and multiplied by 5 to estimate sperm cells in the entire 5 × 5 grid. The distance from the floor of the chamber to the glass coverslip is 0.1 mm. The total volume of the counting area is 10^{-4} cm^3. The dilution factor of the semen to seawater ratio was calculated. The dilution factor was multiplied by the sperm density in the 5 × 5 grid and multiplied by 10^4 to determine the sperm density of the testicular fluid for each male. Each male was counted twice and averaged.

1.2.4 Experiment 1: Effect of pH

At AUSL, the oysters were layered with paper towels, bubble wrap, and ice packs. Thereafter, the oysters were shipped overnight to the Reproductive Physiology Lab, where 4 male oysters (Table 1.2) were processed immediately (5 June 2019). An ASW solution was made with 516 mM NaCl (J.T. Baker, 3627-01), 10.4 mM KCl (VWR Analytical, BDH9258), 11 mM $CaCL_2 \times 2H_2O$ (Ward's Science, 470300-570), 34 mM $MgCl_2 \times 6H_2O$ (EMD Millipore Corp. 442615), and 22 mM $MgSO_4 \times 7H_2O$ (Ward's Science, 470045-528) according to Boulais et al. (2018). When Eastern oyster sperm was diluted in the ASW made according to Boulias et. al (2018), no motility was observed, and the salinity was around approximately 40 PSU. Thus, the ASW was further diluted with ultrapure water (Millipore Direct Q 3 UV) until sufficient sperm activity was observed. The chosen dilution for this experiment was a dilution by half with

ultrapure water to reach a salinity of 20 PSU. Thereafter, the ASW was divided and buffered with either 2-(N-morpholino) ethanesulfonic acid monohydrate (MES) (VWR Life Science, E183), HEPES (VWR Life Science, 0511), or tris (hydroxymethyl)amino-methane (tris) (VWR Life Science, 0497), and all solutions (~100 mL) contained a concentration of 0.4% Pluronic F-127 (Sigma Aldrich, P2443) to prevent cells from sticking to the slides (Alavi et al. 2014). MES (20 mM) was used to buffer pH of 5.0 to 6.0, HEPES (20 mM) was used to buffer a pH of 6.5 to 8.0, and Tris (20 mM) was used to buffer a pH of 8.5 to 11.0. To examine the effects of pH, sodium hydroxide (NaOH) (Fisher Scientific, S318-3) or hydrochloric acid (HCl) (EMD, HX0603-3) was used to adjust pH of ASW between 5.0 and 11.0, in 0.5 increments. In this experiment, percentage of sperm motility and average VCL were analyzed for individual males at 1, 15, 30, 45, and 60 min post-activation.

1.2.5 Experiment 2: Effect of salinity

This experiment was conducted at the AUSL, where semen of 5 males were used (Table 1.2). To make a high salinity stock solution, 1 L of 10 PSU seawater was collected from the broodstock holding system on 14 May 2019. The seawater was boiled on a hot plate until it reached ~40 PSU. This stock solution was then cooled and diluted with ultrapure water to make activating solutions with salinities of 4, 8, 12, 16, 20, 24, 28, and 32 PSU. For each salinity, the osmolality was measured using a Vapor Pressure Osmometer (Table 1.3). A refractometer was used to determine salinities. All solutions contained a concentration of 0.4% pluronic and were buffered with 20 mM Tris to a pH of 8.0 ± 0.2 (based on Section 1.2.4). Due to potential evaporation, salinities were checked and adjusted, if needed, prior to the start of the experiment.

In this experiment, percentage of sperm motility and average VCL were analyzed at 1, 15, 30, 45, and 60 min post-activation.

1.2.6 Experiment 3: Effects of ions

Effects of Ca^{2+} on sperm motility and velocity

Male oysters (n = 4, Table 1.2) were collected from the AUSL on 15 May 2019. An ASW solution was made according to Boulais et al. (2018) and then diluted by half with ultrapure water to reach a salinity of 20 PSU. Additionally, a Ca^{2+} free ASW solution (hereafter, Ca^{2+}-free ASW) was made according to Boulais et al. (2018) and then diluted by half with ultrapure water to reach a salinity of 20 PSU.

The addition of 3 mM ethylene glycol-O,O'-bis(2-aminoethyl)-N,N,N',N'-tetraacetic acid (EGTA) (Alfa Aesar, A16086) was used to chelate out any trace of Ca^{2+} ions in the Ca^{2+}-free ASW. Various concentrations of EGTA were also used to determine how much EGTA is needed to inhibit sperm motility. EGTA was first dissolved in ultrapure water with NaOH to make a stock solution of 100 mM buffered to a pH of 8.0 ± 0.2. The stock solution of EGTA was then added to ASW to make concentrations of 0.5, 1.0, 1.5, 2.0, 2.5, 3.0, and 3.5 mM EGTA.

Three Ca^{2+} channel blockers were used to investigate Ca^{2+} requirements for initiation of sperm motility. Stock solutions of 20 mM mibefradil dihydrochloride hydrate (Sigma, M5441), 500 mM verapamil hydrochloride (AdipoGen, ASG-CR1-3627-G005), and 500 mM nifedipine (Beantown Chemical, 139580) were made. The stock solution for mibefradil was dissolved in ultrapure water, while stock solutions for verapamil and nifedipine were dissolved in dimethyl

sulfoxide (DMSO) (Macron Fine Chemicals, 4948-02). Mibefradil was examined at concentrations of 1, 5, 10, and 50 μM, verapamil at concentrations of 10, 50, 100, and 200 μM, and nifedipine at concentrations of 10, 50, 100, and 200 μM in 20 PSU ASW. The controls for this experiment were ASW, ASW + DMSO, Ca^{2+}-free ASW, and Ca^{2+}-free ASW + DMSO. The DMSO contribution to the control solutions was 0.04% to represent the DMSO level in the highest channel blocker treatments. All solutions contained a concentration of 0.4% Pluronic F-127 and were buffered with 20 mM Tris to a pH of 8.0 ± 0.2. In this experiment, percentage of sperm motility and average VCL were analyzed at 1, 2, 4, 6, 8, 10, 12, 14, 16, 18, and 20 min post-activation.

Effects of K^+, Na^+, and Mg^{2+}on sperm activity

Male oysters (n = 5, Table 1.2) were collected on 27 May 2019 from the Reproductive Physiology Laboratory, previously shipped from AUSL on 26 May 2019. ASW was made (Boulais et al. 2018) and then diluted by half, as above, to reach a salinity of 20 PSU. Additionally, a 100 mL K^+ free ASW (K^+-free ASW) solution was made without KCl (Boulais et al. 2018) and diluted by half to reach a salinity of 20 PSU. Na^+ free ASW (Na^+-free ASW) solution was made without NaCl, which was substituted with 516 mM choline chloride ($C_5H_{14}ClNO$) (Beantown Chemical, 126685) (Boulais et al. 2018) and diluted by half. Mg^{2+} free ASW (Mg^{2+}-free ASW) was made without $MgCl_2 \times 2H2O$ and $MgSO_4 \times 7H2O$, which were substituted with 56 mM choline chloride (Boulais et al. 2018) and diluted by half. The choline chloride was used to maintain the osmolality of the solution (Boulais et al. 2018). To chelate out trace amounts of Mg^{2+}, 1 mM of ethylenediaminetetraacetic acid (EDTA) (VWR Analytical,

BDH9232) was added (Boulais et al. 2018). All of the above activating solutions contained a concentration of 0.4% pluronic by weight and were buffered with 20 mM tris to a pH of 8.0 ± 0.2.

To examine contribution of K^+ and Na^+ fluxes in sperm motility signaling, two K^+ channel blockers and one Na^+ channel blocker were used. Glybenclamide (InvivoGen, tlrl-gly) and 4-aminopyridine (4-AP) (Acros Organics, 504-24-5) were used to block the exchange of K^+ ions, while amiloride hydrochloride dihydrate (ENZO, ALX-550-212-G001) was used to block the exchange of Na^+ ions. Stock solutions of 500 mM glybenclamide, 10 and 2 M 4-AP, and 1 M and 500 mM amiloride were made. Glybenclamide and amiloride were dissolved in DMSO, while 4-AP was dissolved in ultrapure water. The controls for this experiment were ASW, ASW + DMSO, K^+-free ASW, K^+-free ASW + DMSO, Na^+-free ASW, and Na^+-free ASW + DMSO. The DMSO contribution to the control solutions was 1% to represent the DMSO level in the highest channel blocker treatment. Channel blockers were added to ASW and amiloride was also added to Na^+-free ASW solutions. All solutions contained a concentration of 0.4% Pluronic F-127 and were buffered with 20 mM Tris to a pH of 8.0 ± 0.2. In this experiment, percentage of sperm motility and average VCL were analyzed at 1, 5, 15, 30, 45, and 60 min post-activation.

1.2.7 Statistical analyses

Data were analyzed using SAS statistical analysis software (v. 9.1; SAS Institute Inc., Cary, NC, USA). Residuals were tested for normality (Shapiro–Wilk test) and homogeneity of variance (plot of residuals vs. predicted values). Velocity data were $\log_{10}$ transformed, while percent sperm motility data were arcsine square-root transformed to meet assumptions of

normality and homoscedasticity when necessary. The Kenward–Roger procedure was used to approximate denominator degrees of freedom for all F-tests (Spilke et al. 2005). Error bars represent least square means standard error. To examine the effect of pH, salinity, ions, and channel blockers on sperm motility and velocity, data were analyzed using a series of repeated measures factorial ANOVA models. Each model contained the activation media (including pH, salinity, ions, or channel blockers) and post-activation time, as well as the corresponding activation media × post-activation time interaction. In the case of a significant interaction, the models were decomposed into individual one-way ANOVA models at each post-activation time. These revised models involved only preplanned comparisons and did not include repeated use of the same data, so α-level corrections for a posteriori comparison were not necessary. If a non-significant interaction was detected the main effects of activation media (including pH, salinity, ions, or channel blockers) and time were interpreted. Treatment means were contrasted using the Tukey's test. Alpha was set at 0.05 for main effects and interactions.

1.3 Results

Testicular fluid of the Eastern oyster (n = 5) was sampled to determine the pH and osmolality (mOsmol/kg) (Table 1.1). The average pH and osmolality of the testicular fluid was 5.8 ± 0.04 and 569.60 ± 34.60 mOsmol/kg, respectively (Table 1.1). For each experiment, male oyster morphometrics including length (mm), width (mm), height (mm), weight (g), and sperm density (cells/mL) were recorded (Table 1.2). Sperm densities of individuals ranged from 9.40×10^8 to 5.53×10^{10} cells/mL (Table 1.2).

1.3.1 Experiment 1: Effect of pH

Sperm motility and velocity were activated across a wide range of pH treatments (Figs. 1.1 and 1.2). No sperm activity was observed at a pH of 5.0, 5.5, 6.0, or 11.0, and these treatments were not included in the statistical analysis. Since these sperm traits were evaluated at various pH and post-activation times, the interaction between pH and time was statistically analyzed, which showed no significant effects for motility or velocity ($P = 0.5178$) (Figs. 1.1A and 1.2A). Therefore, the main effects of pH (Figs. 1.1B and 1.2B) and time (Figs. 1.1C and 1.2C) were interpreted.

The results showed that pH significantly affected sperm motility with highest values observed after activation of sperm in ASW with pH treatments ranging from 7.5 to 10.0 ($P < 0.0001$) (Fig. 1.1B). However, sperm motility did not show significant differences at different times post-activation ($P = 0.4850$) (Fig. 1.1C). To determine which pH gave the highest sperm motility, a series of regression functions were generated that show motility at the different post-activation times for each pH. The regressions were nonlinear second-order polynomial dome-shaped functions (Table 1.4, Fig. 1.1D). Setting the derivative to zero provided the pH at which the highest motility was obtained. Based on this function, the highest sperm motilities were observed between pH 8.66 to 8.83 from 1 to 60 min post-activation (Table 1.4). Sperm head trajectories were circular for every pH, indicating that flagellar beating was asymmetric (Fig. 1.1E).

Similar to sperm motility, pH significantly affected sperm velocity with highest values observed after activation of sperm in ASW with pH ranging from 7.5 to 10.0 ($P < 0.0001$) (Fig. 1.2B). Sperm velocity was significantly different at the various post-activation times ($P =$

0.0143) (Fig. 1.2C), where a significant decrease in sperm velocity was observed at 30 min post-activation (Fig. 1.2C). To determine the pH in which gave the highest sperm velocity, a series of regressions were generated at each post-activation time. The regressions were again nonlinear second-order polynomial dome-shaped functions (Table 1.4, Fig. 1.2D), showing highest sperm velocity between pH 8.83 to 9.09 from 1 to 60 min post-activation.

Together, these results show that the Eastern oyster sperm requires an alkaline condition to exhibit the highest sperm motility (pH from 8.66 to 8.83) and velocity (pH from 8.83 to 9.09) after dilution with seawater.

1.3.2 Experiment 2: Effect of salinity

Sperm motility was initiated across a wide range of salinity treatments between 4 and 32 PSU (Fig. 1.3). Interactions between salinity and time were statistically analyzed for motility and velocity, which showed no significant effects ($P = 0.9759$) (Figs. 1.3A and 1.4A). Therefore, the main effects of pH (Figs. 1.3B and 1.4B) and time (Figs. 1.3C and 1.4C) were interpreted.

The results showed that salinity significantly affected sperm motility with highest values observed after activation in ASW with salinity ranging from 12 to 20 PSU ($P < 0.0001$) (Fig. 1.3B). Sperm motility was not triggered in ASW with a salinity of 4 and 32 PSU (Fig. 1.3B). Sperm motility was significantly different at different post-activation times ($P = 0.0028$) (Fig. 1.3C), where a significant increase in motility was observed at 15 min post-activation relative to 1 min post-activation, with no significant differences among any other time tested. To determine which salinity initiated the highest sperm motility, a series of regressions were generated at each post-activation time for each salinity. The regressions were nonlinear second-order polynomial

dome-shaped functions (Table 1.4, Fig 1.3D), showing highest motility between salinity 16.83 and 17.91 from 1 to 180 min post-activation. Sperm head trajectories were circular for all salinities, indicating that flagellar beating was asymmetric (Fig. 1.3E).

Similar to sperm motility, salinity significantly affected sperm velocity with highest values observed after activation of sperm in ASW with salinities ranging from 12 to 24 PSU ($P < 0.0001$) (Fig. 1.4B). Sperm velocity was significantly different at different time post-activation ($P < 0.0001$) (Fig. 1.4C), where a significant increase in sperm velocity was observed at 4 min post-activation with highest values recorded at 8 min and 10 min post-activation (Fig. 1.4C). Regression functions were generated at the various post-activation times for each salinity. Here, nonlinear second-order polynomial dome-shaped functions were observed (Table 1.4, Fig 1.4D), where the highest velocities were observed between salinities of 16.50 and 18.32 PSU from 1 to 180 min post-activation.

These results show that Eastern oyster sperm motility was highest in salinities between 12 and 24 PSU and fully suppressed at 4 and 32 PSU.

1.3.3 Experiment 3: Effects of ions

Effects of Ca^{2+} on sperm motility and velocity

The interaction between Ca^{2+} treatments and time was statistically analyzed for sperm motility and velocity, which showed significant effects (P = 0.0006). Therefore, sperm motility and velocity were statistically analyzed at each post-activation time [Figs. 1.5 and 1.6 and Supplementary Figs. 1.1 and 1.2; all significant P-valves (< 0.0001) except for VCL at 1 (P = 0.0804) and 2 min (P = 0.05)].

Sperm motility was initiated in Ca^{2+}-free ASW at 1 and 2 min post-activation, with no significant differences compared to that of ASW. However, sperm motility significantly decreased in Ca^{2+}-free ASW at 4 min post-activation (Supplementary Fig. 1.1). At 1 min post activation, sperm motility decreased in ASW containing 10 and 50 μM mibefradil or 100 μM verapamil (Fig. 1.5). At 2 min post-activation, sperm motility decreased in 10 and 50 μM mibefradil or 200 μM verapamil (Supplementary Fig. 1.1). At 4 min post-activation, sperm motility was totally suppressed in 50 μM mibefradil and significantly decreased in ASW containing 10 μM mibefradil (Supplementary Fig. 1.1). At 6 min post-activation, sperm motility significantly decreased in ASW containing 10 μM mibefradil or 50, 100, and 200 μM verapamil (Supplementary Fig. 1.1). At 8 min post-activation, sperm motility was totally suppressed in ASW containing 10 μM mibefradil and significantly decreased in ASW containing 10, 50, 100, and 200 μM verapamil (Supplementary Fig. 1.1). The suppression effects of 10 or 50 μM mibefradil and inhibitory effects of 10, 50, 100, or 200 μM verapamil on sperm motility initiation were observed at 10, 12, 14, 16, 18, and 20 min post-activation (Fig. 1.5 and Supplementary Fig. 1.1). However, nifedipine (10 to 200 μM) had no effect on sperm motility evaluated at any post-activation time (Fig. 1.5 and Supplementary Fig. 1.1).

Sperm velocity was also not significantly different in ASW compared to Ca^{2+}-free ASW at 1 and 2 min post-activation (Fig. 1.6 and Supplementary Fig. 1.2). However, velocity

decreased in Ca^{2+}-free ASW at 4 min post-activation. The Ca^{2+} channel blockers (1 to 50 μM mibefradil and 10 to 200 μM verapamil) were also without significant effects on sperm velocity at 1 and 2 min post-activation. By 4 min post-activation, sperm velocity decreased in ASW containing 10 mibefradil or 100 and 200 μM verapamil (Supplementary Fig. 1.2). At 8 and 10 min post-activation, respectively, sperm velocity decreased in ASW containing 50 and 10 μM verapamil (Fig. 1.6 and Supplementary Fig. 1.2). Nifedipine did not impact sperm velocity at all concentrations (10, 50, 100, and 200 μM) and post-activation times (Fig. 1.6 and Supplementary Fig. 1.2).

For sperm motility, the interaction between EGTA and post-activation time was significant ($P = 0.0080$), thus data were statistically analyzed at each post-activation time (Figs. 1.7A-C and Supplementary Fig. 1.3). Sperm motility was initiated in ASW containing 0.5 to 3.5 mM EGTA. At 1 and 2 min post-activation motility values were similar across the EGTA gradient (Fig. 1.7 and Supplementary Fig. 1.3; $P > 0.3044$). Thereafter, EGTA concentration had a significant impact on motility ($P < 0.0121$), where it was totally suppressed in ASW containing 3.0 or 3.5 mM EGTA after 6 min post-activation (Fig. 1.7 and Supplementary Fig. 1.3). Within 20 min post-activation, sperm motility in ASW containing 0.5 to 2.5 mM EGTA was not different.

For sperm velocity, the interaction effect was not significant ($P = 0.0893$; Fig. 1.7D), thus the main effects of EGTA (Fig. 1.7E) and time (Fig. 1.7F) were interpreted. Significant decreases in sperm velocity were observed in ASW containing 2.5, 3.0, and 3.5 mM EGTA ($P < 0.0001$; Fig. 1.7E). There was also a significant impact of time on sperm velocity in ASW containing various concentrations of EGTA ($P = 0.0007$), such that sperm velocity was highest at 2 min compared to 6, 10, and 16 min (Fig. 1.7F).

Taken together, inhibition of sperm motility in ASW containing EGTA or in Ca^{2+}-free ASW suggests that Ca^{2+} ions are required for initiation of motility. Inhibition or suppression of sperm motility in ASW containing mibefradil and verapamil suggest Ca^{+} influx is essential for sperm motility initiation. A decrease in sperm velocity in Ca^{2+}-free ASW or in ASW containing EGTA, mibefradil, or verapamil suggest that Ca^{2+} ions are involved in flagellar beating force.

Effects of K^{+} on sperm motility and velocity

For sperm motility, the interaction between treatments and post-activation time was not significant ($P = 0.0830$; Fig. 1.8A), thus the main effects of K^{+} treatments (Fig. 1.8B) and post-activation time (Fig. 1.8C) were interpreted. There was a significant impact of K^{+} treatments ($P < 0.0001$), such that sperm motility was decreased in K^{+}-free ASW, ASW containing 10 and 50 mM 4-AP, and ASW containing 500 mM glybenclamide (Fig. 1.8B). Inhibitory effects of 4-AP and glybenclamide were concentration-dependent. However, there was no significant impact of post-activation time ($P = 0.1360$; Fig. 1.8C).

For sperm velocity, the interaction between K^{+} treatments and post-activation time was significant ($P < 0.0001$). Therefore, the effects of K^{+} were analyzed at each post-activation time (Fig. 1.8D-I, all $P < 0.0105$). In K^{+}-free ASW, sperm velocity significantly decreased at ≥ 15 min post-activation. In ASW containing 4-AP, a significant decrease in sperm velocity was observed at ≥ 10 mM at 1 min post-activation and 50 mM at 5 and 15 min post-activation. However, there was no significant difference in sperm velocity in ASW containing 50, 200, or 500 mM glybenclamide within 60 min post-activation (Fig. 1.8D-I).

Effects of Na^+ on sperm motility and velocity

The interaction was non-significant for sperm motility ($P = 0.4769$; Fig. 1.9A) and velocity ($P = 0.2072$; Fig. 1.9D). Thus, the main effects of Na^+ treatments (Fig. 1.9B and 1.9E) and post-activation time (Fig. 1.9C and 1.9F) were interpreted. There was a significant impact of Na^+ ions on sperm motility (Fig. 1.9B) and velocity (Fig. 1.9E) ($P < 0.0001$). Both sperm motility and velocity were decreased in Na^+-free ASW and in ASW containing ≥ 0.02 mM amiloride ($P < 0.0001$). There was no significant impact of post-activation time on sperm motility ($P = 0.4728$; Fig. 1.9C) and sperm velocity ($P = 0.1114$; Fig. 1.9F).

Effects of Mg^{2+} on sperm motility and velocity

The interaction between treatments and post-activation time was non-significant for both sperm motility ($P = 0.6518$; Fig. 1.10A) and velocity ($P = 0.3974$; Fig. 1.10D). Thus, the main effects of Mg^{2+} ions (Fig. 1.10B and 1.10E) and post-activation time (Fig. 1.10C and 1.10F) were interpreted. There was a significant impact of treatment, such that sperm motility was lower with Mg^{2+}-free ASW compared to ASW ($P = 0.0027$; Fig. 1.10B), while velocity did not differ significantly ($P = 0.0578$; Fig. 1.10E). Moreover, there was no significant impact of time post-activation on sperm motility ($P = 0.0612$; Fig. 1.10C) and sperm velocity ($P = 0.9317$; Fig. 1.10F).

1.4 Discussion

Although the molecular structure of the motility apparatus is evolutionarily conserved in sperm of animals (Inaba 2011), the signal molecules that regulate sperm motility initiation are diverse and complex (Darszon et al. 1999; Wachten et al. 2017; Alavi et al. 2019). In this context, sperm motility signaling is largely unknown in bivalve mollusks and limited to species that inhabit aquatic environments with a salinity of full-strength seawater (Boulais et al. 2019). In the present study, we investigated the effects of salinity on sperm motility and velocity in the Eastern oyster, an euryhaline bivalve. Sperm motility was initiated at a salinity ranging from 8 to 28 PSU and was totally suppressed at a salinity of 32 PSU. Thereafter, the physiological roles of pH and ions on sperm motility initiation and their impacts on sperm velocity were studied at a salinity of 20 PSU to elucidate whether sperm motility signaling differs from other bivalve species that spawn in normal seawater. Sperm motility was inhibited in ASW with a pH of ≤ 7.0, and in Ca^{2+}-(except for 1 min post-activation), Na^{+}-, K^{+}-, and Mg^{2+}-free ASW, all of which were associated with decreases in sperm velocity, except for Mg^{2+}-free ASW. Further experiments using Ca^{2+}, Na^{+}, and K^{+} channel blockers showed that Ca^{2+} and Na^{+} influxes and K^{+} efflux occur upon initiation of sperm motility.

Our results showed that the salinity of activation media significantly affects sperm motility and velocity. We observed that motility of the Eastern oyster sperm was initiated in salinities between 8 and 28 PSU. The optimal salinities in which the highest sperm motilities were observed (12 to 24 PSU) had an osmolality of 241.33 to 527.67 mOsmol/kg, respectively. Considering the osmolality of the testicular fluid in Eastern oyster was 569.60 ± 34.60 mOsmol/kg (Table 1.2), these results show that the osmolality in which sperm motility was

initiated is lower to that of testicular fluid. Similarly, Boulais et al. (2018) reported that osmolality of the testicular fluid in the Pacific oyster (1060 mOsmol/kg) is close to that of seawater. They also reported that sperm motility was triggered in salinities between 14 to 50 PSU with the highest motility observed from 19.3 to 42.7 PSU at 5 min post-activation (Boulais et al. 2018). Dong et al. (2002) also reported that sperm motility in the Pacific oyster was triggered in osmolalities between 400 and 1400 mOsmol/kg with the highest motility observed in 800-1100 mOsmol/kg. Therefore, osmolality of the seminal plasma is not an inhibitory factor to maintain sperm in the quiescent state in the reproductive organ. Moreover, we observed that sperm motility was not initiated in a 500 mOsmol /kg glucose solution (unpublished data) similar to previous reports on the Pacific oyster, Japanese scallop, and Manila clam (Alavi et al. 2014). Together, these findings confirm that sperm motility initiation in bivalves is osmolality-independent.

It has been documented that testicular fluid exhibits acidic pH which helps to maintain sperm in the quiescent state in the reproductive organ of many bivalve species, including Pacific oyster, Japanese oyster, European flat oyster, great scallop, and black-lip pearl oyster (Faure et al. 1994; Demoy-Schneider et al. 2012; Alavi et al. 2014; Boulais et al. 2018). Similarly, we observed that pH of the testicular fluid is acidic in the Eastern oyster sperm (pH 5.8 ± 0.04; Table 1.1), and sperm motility was not activated in ASW buffered to a low pH of 5.0, 5.5, or 6.0. However, motility was triggered in 5.17 ± 3.75% of sperm at pH of 6.5 and was highest at pH 7.5 to 10.0. Similarly, it has been reported that an acidic pH of 6.0 to 7.0 inhibits sperm motility initiation, and the highest percentage of sperm become motile at alkaline pH ranging from 7.5 to 11.5 in the black-lip pearl oyster, Japanese pearl oyster, Pacific oyster, Japanese scallop, and Manila clam (Alavi et al. 2014; Boulais et al. 2018). Testicular fluid pH is lower than the pH of

ASW in which sperm motility is initiated, and thus suggests that pH maintains sperm in the quiescent state in the reproductive organ before spawning. Our study suggests that once sperm is released from the acidic testicular fluid environment to the alkaline seawater at spawning, sperm motility is initiated, which is associated with an influx of proton ions (Alavi et al. 2004; Boulais et al. 2018). It is worth to note that a very old study has reported that low environmental pH decreases reproductive success in the Eastern oyster (Prytherch 1928). Although the Eastern oyster will spawn in seawater with a pH of 6.0 to 10.0, the sperm and oocytes lose their viability within 2 to 4 h outside of this range (Calabrese and Davis 1966, 1969, 1970). Therefore, based on our study, it is recommended to maintain a pH of 7.5 or greater when spawning the Eastern oyster to ensure optimal sperm activation and performance.

Sperm motility in the Eastern oyster was inhibited in Ca^{2+}-free ASW, or ASW containing EGTA, confirming statements from Alavi et al. (2014) that sperm motility longevity in bivalves is Ca^{2+}-dependent. Our results showed that sperm motility in the Eastern oyster was totally suppressed at 3.0 to 3.5 mM EGTA at 4 min post-activation and thereafter. However, sperm motility was suppressed at 5, 10, and 5 mM EGTA in Pacific oyster, Japanese scallop and Manila clam, respectively (Alavi et al. 2014; Boulais et al. 2018). These findings may suggest that there is a species-specific requirement to extracellular Ca^{2+} concentrations. Inhibition or suppression of sperm motility initiation in the presence of mibefradil or verapamil also indicate that sperm of the Eastern oyster, similar to other bivalve species (Alavi et al. 2014), requires Ca^{2+} ion influx for the maintenance of motility. Our results found that nifedipine (10, 50, 100, and 200 μM) had no effect on sperm motility in the Eastern oyster. However, Alavi et al. (2014) reported that nifedipine is capable of inhibiting sperm motility initiation in the Japanese scallop. This difference may be due to species-specific tolerances to channel blockers, suggesting the

presence of species-specific types of Ca^{2+} channels (Kho et al. 2004; Alavi et al. 2014); however, the molecular identity of Ca^{2+} channels are completely unknown in bivalves.

Our results showed that motility for Eastern oyster sperm was decreased in K^+-free ASW, suggesting K^+ transport through ion channels is part of the mechanism behind sperm activation. For the Japanese scallop and Pacific oyster, sperm motility was initially activated in K^+-free seawater (Alavi et al. 2014; Boulais et al. 2018); however, motility was decreased within 60 min post-activation in the Japanese scallop. Inhibition of sperm motility in K^+-free ASW suggests that K^+ ions are important to create an optimal condition for maintenance of sperm motility in marine bivalve mollusks, similar to that of sea urchin (Christen et al. 1986; Alavi et al. 2014). Similar to Japanese scallop sperm (Alavi et al. 2014), our results also showed that motility of Eastern oyster sperm was decreased in ASW containing K^+ channel blockers, 4-AP and glybenclamide, suggesting that K^+ efflux through a voltage-dependent K^+ channel is essential for initiation of sperm motility. The efflux of K^+ ions has also been reported upon sperm motility initiation in mammals, human, fish, ascidian, and sea urchin (Rothschild 1948; Jones 1978; Johnson et al. 1983; Morisawa et al. 1983b; Izumi et al. 1999; Krasznai et al. 2000).

Our study found that sperm motility imitation was lower in Na^+-free ASW than that of ASW, suggesting that extracellular Na^+ plays a role in sperm motility signaling. Similarly, other studies found that motility was suppressed in Na^+-free seawater for the Manila clam, Japanese scallop, and Pacific oyster (Faure et al. 1994; Alavi et al. 2014; Boulais et al. 2018). These studies suggest that the exchange of external Na^+ ions through Na^+/K^+-ATPase pumps or Na^+/H^+ exchangers regulates intracellular pH; causing an alkalization that is required for the initiation of sperm motility (Gatti and Christen 1985; Boulais et al. 2019). It is worth to note that Na^+ ions may contribute to regulation of intracellular Ca^{2+} ions via Na^+/Ca^{2+} exchanger (Vines et al. 2002;

Shiba et al. 2006; Alavi et al. 2014). Our results showed that amiloride did not affect sperm motility of the Eastern oyster, except when added into Na^+-free ASW. This is likely due to the fact that Na^+-free ASW already caused a significant decrease in motility when compared to ASW even though amiloride was present.

Out of all the ions free ASW solutions, Mg^{2+}-free ASW showed a smaller impact on sperm motility. Boulais et al. (2018) found similar results in the Pacific oyster, where neither motility nor velocity was impacted with Mg^{2+}-free ASW. Based on our results and other studies, it seems that while the presence of Mg^{2+} ions in seawater can improve motility for some bivalves, Mg^{2+} ions are not involved in sperm motility.

Consistent with previous studies on Pacific oyster sperm (Boulais et al. 2018), sperm velocity was seen to be lower at pH ≤ 7.0 suggesting that alkaline conditions are required for dynein ATPase activity (Christen et al. 1982; Boitano and Omoto 1991; Nakajima et al. 2005). We also observed that sperm velocity was decreased in K^+-free ASW or in ASW containing 4-AP which was consistent with a previous study on Japanese scallop sperm (Alavi et al. 2014). These results suggest that K^+ ions might be involved in the regulation of axonemal beating force via alkalization of intracellular pH. Sperm velocity in the Eastern oyster was also decreased in Ca^{2+}-free ASW, ASW containing EGTA, mibefradil, and verapamil, similarly to other bivalve species (Alavi et al. 2014), suggesting that Ca^{2+} ions are involved in the flagellar beating force. Sperm velocity was decreased in Na^+-free ASW, however it was higher in sperm activated in ASW containing amiloride than Na^+-free ASW with or without amiloride. Together, these findings suggest that Na^+ ions are involved in regulation of flagellar beating force mediated by intracellular pH or intracellular Ca^{2+} concentrations (Alavi et al. 2014; Boulais et al. 2018).

1.5 Conclusions

Overall, our results show that manipulating the physical and chemical components of seawater can affect sperm performance in the Eastern oyster. This study reveals insights into the cellular processes behind motility initiation and provides vital information which can be used by hatcheries to improve male performance and artificial fertilization in a bivalve species of upmost economic importance. Figure 1.11 illustrates the signaling pathways investigated in this study which are responsible for triggering sperm motility initiation in bivalves. Sperm released into alkaline seawater results in an influx of Na^+ ions and efflux of H^+ protons facilitated a Na^+-dependent alkalization of internal pH triggering motility initiation. Moreover, K^+ efflux through voltage-dependent K^+ channels generates hyperpolarization of sperm membrane potential. Under alkaline conditions, voltage-dependent Ca^{2+} channels open, allowing for Ca^{2+} influx which triggers Ca^{2+}/calmodulin-dependent flagellar beating. Ultimately, this information can be used to create short-term storage media, where dilution of sperm into (i) media close to the pH of testicular fluid (5.8), (ii) media with a high concentration of K^+ ions, and (iii) media without Na^+ and Ca^{2+} ions would help maintain sperm in the quiescent state. Additionally, our findings can be used to assist in the development of long-term storage media for cryopreservation where sperm-activating ions must be excluded.

This study has implications that surpass the scope of assisted reproduction into a more comprehensive understanding of the natural ecology of the Eastern oyster. The effects of climate change such as ocean warming, and ocean acidification are projected to increase overtime. This species has a pH-dependent reproductive strategy, and deviations to ocean pH could be catastrophic to wild oyster populations reguarding larval recruitment. Additionally, this species

inhabits brackish water that experiences changes in pH and salinity naturally lower than the open ocean. Wild oysters that spawn in seawater with a pH lower than 7.0 and salinity less than 12 PSU will most likely experience poor fertilization success and larval survival. Our study provides ecologists with valuable information to better predict how changes in the ocean will impact oyster spawning dynamics. Ultimately, the Eastern oyster can be used as a model organism to understand reproductive physiology of other estuarine species and marine bivalves around the world.

Finally, our results show that the Eastern oyster sperm becomes motile at salinities ranging from 8 to 28 PSU and suppressed at salinities ≤ 4 and ≥ 32 PSU. Sperm motility is initiated at an alkaline pH and requires extracellular Na^+, K^+, and Ca^{2+} ions. Removing these ions from ASW results in inhibition of sperm motility and a decrease in sperm velocity. Considering the salinity of the aquatic environment in which the Eastern oyster spawn (5 to 40 PSU) (Galtsoff 1964; Wallace 1966), comparisons of sperm motility signaling with bivalve species inhabiting normal seawater (35 PSU) show that (i) initiation of sperm motility is osmolality-independent in both groups, however salinity highly affects the percentage of motile sperm and sperm velocity and (ii) sperm motility signaling is well conserved, as it occurs at alkaline pH and requires Na^+ and K^+ efflux and Ca^{2+} influx. However, molecular identification and characterization of specific ion channels remain to be elucidated in further studies, as sperm motility or velocity exhibits concentration-dependent differences to extracellular ions and ion channel blockers.

Acknowledgements

This work was supported by the Alabama Agriculture Experimental Station & the USDA National Institute of Food & Agriculture, Hatch project (1013854).

References

Alavi, S. M. H., and J. Cosson. 2005. Sperm motility in fishes. I. Effects of temperature and pH: A review. Cell Biology International 29(2):101-110.

Alavi, S. M. H., and J. Cosson. 2006. Sperm motility in fishes. (II) Effects of ions and osmolality: A review. Cell Biology International 30(1):1-14.

Alavi, S. M. H., J. Cosson, O. Bondarenko, and O. Linhart. 2019. Sperm motility in fishes: (III) diversity of regulatory signals from membrane to the axoneme. Theriogenology 136:43-165.

Alavi, S. M. H, J. Cosson, M. Karami, B. M. Amiri, and M. A. Akhoundzadeh. 2004. Spermatozoa motility in the Persian sturgeon, *Acipenser persicus*: Effects of pH, dilution rate, ions and osmolality. Reproduction 128(6):819-828.

Alavi, S. M. H., O. Linhart, K. Coward, M. Rodina. 2008. Fish spermatology: implication for aquaculture management. In: Alavi, S. M. H., J. Cosson, K. Coward, G. Rafiee (eds) Fish Spermatology. Alpha Science International Ltd., Oxford, pp 397-460.

Alavi, S. M. H., N. Matsumura, K. Shiba, N. Itoh, K. G. Takahashi, K. Inaba, and M. Osada. 2014. Roles of extracellular ions and pH in 5-HT-induced sperm motility in marine bivalve. Reproduction 147(3):331-345.

Billard, R. 1978. Changes in structure and fertilizing ability of marine and freshwater fish spermatozoa diluted in media of various salinities. Aquaculture 14:187-198.

Billard, R. 1983. Ultrastructure of trout spermatozoa: Changes after dilution and deep-freezing. Cell and Tissue Research 228:205-218.

Billard, R., J. Cosson, G. Perchec, and O. Linhart. 1995. Biology of sperm and artificial reproduction in carp. Aquaculture 129:95-l12.

Bobe, J., and C. Labbé. 2010. Egg and sperm quality in fish. General and Comparative Endocrinology 165(3):535-548.

Boitano, S., and C. K. Omoto. 1991. Membrane hyperpolarization activates trout sperm without an increase in intracellular pH. Journal of Cell Science 98:343-349.

Boulais, M., M. Demoy-Schneider, S. M. H. Alavi, and J. Cosson. 2019. Spermatozoa motility in bivalves: Signaling, flagellar beating behavior, and energetics. Theriogenology 136:15-27.

Boulais, M., M. Suquet, E. J. Arsenault-pernet, F. Malo, I. Queau, P. Pignet, D. Ratiskol, J. Le Grand, M. Huber, and J. Cosson. 2018. pH controls spermatozoa motility in the Pacific oyster (*Crassostrea gigas*). Biology Open 7:bio031427.

Butts, I. A. E., S. M. H. Alavi, A. Mokdad, and T. E. Pitcher. 2013. Comparative Biochemistry and Physiology, Part A Physiological functions of osmolality and calcium ions on the initiation of sperm motility and swimming performance in redside dace, *Clinostomus elongatus*. Comparative Biochemistry and Physiology, Part A 166(1):147-157.

Butts, I. A. E., M. K. Litvak, and E. A. Trippel. 2010. Seasonal variations in seminal plasma and sperm characteristics of wild-caught and cultivated Atlantic cod, *Gadus morhua*. Theriogenology 73:873-885.

Butts, I. A. E., E. A. Trippel, A. Ciereszko, C. Soler, M. Słowińska, S. M. H. Alavi, M. K. Litvak, and I. Babiak. 2011. Seminal plasma biochemistry and spermatozoa characteristics of Atlantic cod (*Gadus morhua* L.) of wild and cultivated origin. Comparative Biochemistry and Physiology, Part A 159:16-24.

Calabrese, A. and H. C. Davis. 1966. The pH tolerance of embryos and larvae of *Mercenaria mercenaria* and *Crassostrea virginica.* Biological Bulletin 131:427-436.

Calabrese, A. and H. C. Davis. 1969. Spawning of the American oyster, *Crassostrea virginica,* at

extreme pH levels. Veliger 11:235-237.

Calabrese, A. and H. C. Davis. 1970. Tolerances and requirements of embryos and larvae of bivalve mollusks. Helgoländer wiss. Meeresunters 20:553-564.

Chanley, P. E. 1958. Survival of some juvenile bivalves in water of low salinity. Proceedings of the National Shellfisheries Association 48:52-65.

Christen, R., R. W. Schackmann, and B. M. Shapiro. 1982. Elevation of the intracellular pH activates respiration and motility of sperm of the sea urchin, *Strongylocentrotus purpuratus*. Journal of Biological Chemistry 257(24):14881-14890.

Christen, R., R. W. Schackmann, and B. M. Shapiro. 1983. Metabolism of Sea Urchin Sperm. The American Naturalist 83(813):285-301.

Christen, R., R. W. Schackmann, and B. M. Shapiro. 1986. Ionic regulation of sea urchin sperm motility, metabolism and fertilizing capacity. The Journal of Physiology 379:347-365.

Cosson, J. 2008. Methods to analyze the movements of the spermatozoa and their flagella. In: Alavi, S. M. H., J. Cosson, K. Coward, G. Rafiee (eds) Fish Spermatology. Alpha Science Ltd. Oxford, UK, pp. 63-102.

Cosson J. 2015. Flagellar mechanics and sperm guidance. Bentham Science Publishers, Sharjah, UAE pp. 1-445.

Cosson, J., A. L. Groison, M. Suquet, C. Fauvel, C. Dreanno, and R. Billard. 2008. Studying sperm motility in marine fish: An overview on the state of the art. Journal of Applied Ichthyology 24(4):460-486.

Darszon, A., P. Labarca, T. Nishigaki, and F. Espinosa. 1999. Ion channels in sperm physiology. Physiological Reviews 79(2):481-510.

Demoy-Schneider, M., A. Levêque, N. Schmitt, Le Pennec, J. Cosson, M. L. Pennec, and J.

Cosson. 2012. Motility activation and metabolism characteristics of spermatozoa of the black-lip-pearl oyster *Pinctada margaritifera* var: *Cumingii* (Jameson, 1901). Theriogenology 77(1):53-64.

Demoy-Schneider, M., N. Schmitt, M. Suquet, C. Labbé, M. Boulais, G. Prokopchuk, and J. Cosson. 2014. Biological characteristics of sperm in two oyster species: The pacific oyster, *Crassostrea gigas*, and the black-lip pearl oyster, *Pinctada margaritifera*. In: Erickson, B. T. (ed), Spermatozoa. Biology, Motility and Function and Chromosomal Abnormalities. Nova Science Publishers, Incorporated, Hauppauge, USA, 259 pp. 15-74.

Dinnel, P. A., J. M. Link, and Q. J. Stober. 1987. Improved methodology for a sea urchin sperm cell bioassay for marine waters. Archives of Environmental Contamination and Toxicology 16(1):23-32.

Dong, Q., T. R. Tiersch, B. Eudeline, and S. K. Allen. 2002. Factors affecting sperm motility of tetraploid Pacific oysters. Journal of Shellfish Research 21(2):719–723.

Drinkwater, M., Y. Kerr, J. Font, and M. Berger. 2009. Exploring the water cycle of the 'blue planet' The soil moisture and ocean salinity (SMOS) mission. European Space Agency Bulletin 137.

Dzyuba, V., and J. Cosson. 2014. Motility of fish spermatozoa: From external signaling to flagella response 14(3):165-75.

Ewart, J. W. and S. E. Ford. 1993. History and impact of MSX and Dermo diseases on oyster stocks in the Northeast Region. Northeastern Regional Aquaculture Center Fact Sheet no. 200. University of Massachusetts Dartmouth, North Dartmouth, Massachusetts.

Faure, C., N. Devauchelle, and J. P. Girard. 1994. Ionic factors affecting motility, respiration and

fertilization rate of the sperm of the bivalve *Pecten maximus* (L.). Journal of Comparative Physiology B 164(6):444-450.

FAO. 2018. The State of World Fisheries and Aquaculture 2018 - Meeting the sustainable development goals. Rome. License: CC BY-NC-SA 3.0 IGO.

The Ford, S. E. and M. R. Tripp. 1996. Diseases and defense mechanisms. In: Kennedy, V.S., R. I. E. Newell, and A. F. Eble (eds) The Eastern Oyster *Crassostrea virginica*. Maryland Sea Grant College, College Park, Maryland, pp. 581-660.

Galtsoff, P. S. 1964. The American Oyster *Crassostrea virginica* Gmelin. Fishery Bulletin. In: Fishery Bulletin. US Government Printing Office, Washington, DC, USA, pp. 64:1-480.

Gatti, J. L., and R. Christen. 1985. Regulation of internal pH of sea urchin sperm. Journal of Biological Chemistry 260(12):7599–7602.

Inaba, K. 2011. Sperm flagella: Comparative and phylogenetic perspectives of protein components. Molecular Human Reproduction 17(8):524–538.

Izumi, H., T. Marian, K. Inaba, Y. Oka, and M. Morisawa. 1999. Membrane hyperpolarization by sperm-activating and -attracting factor increases cAMP level and activates sperm motility in the ascidian, *Ciona intestinalis*. Developmental Biology 213:246–256.

Jackson, J. B. C., M. X. Kirby, W. H. Berger, K. A. Bjorndal, L. W. Botsford, B. J. Bourque, R. H. Bradbury, R. Cooke, J. Erlandson, J. A. Estes, T. P. Hughes, S. Kidwell, C. B. Lange, H. S. Lenihan, J. M. Pandolfi, C. H. Peterson, R. S. Steneck, M. J. Tegner, and R. R. Warner. 2001. Historical overfishing and the recent collapse of coastal ecosystems. Science 293(5530):629-637.

Johnson, C. H., D. L. Clapper, M. M. Winkler, H. C. Lee, and D. Epel. 1983. A volatile inhibitor immobilizes sea urchin sperm in semen by depressing the intracellular pH. Developmental

Biology 98(2):493-501.

Jones, R. 1978. Comparative biochemistry of mammalian epididymal plasma. Comparative Biochemistry and Physiology Part B: Biochemistry 61(3):365-370.

Kennedy, V. S. 1996. The ecological role of the Eastern oyster, *Crassostrea virginica*, with remarks on disease. Journal of Shellfish Research 15:177-183.

Kho, K. H., S. Tanimoto, K. Inaba, Y. Oka, and M. Morisawa. 2004. Transmembrane cell signaling for the initiation of trout sperm motility: roles of ion channels and membrane hyperpolarization for cyclic AMP synthesis. Zoological Science 18(7):919-928.

Kime, D. E., M. Ebrahimi, K. Nysten, I. Roelants, E. Rurangwa, H. D. M. Moore, and F. Ollevier. 1996. Use of computer assisted sperm analysis (CASA) for monitoring the effects of pollution on sperm quality of fish; application to the effects of heavy metals. Aquatic Toxicology 36:223-237.

Kinnby, A., K. Johannesson, and J. Havenhand. 2015. Effects of reduced salinity on fertilization and larval development in the Pacific oyster, *Crassostrea gigas* (Thunberg, 1789). Master of Science Thesis. Department of Biological and Environmental Sciences, University of Gothenburg.

Krasznai, Z., L. Balkay, T. Márián, L. Trón, and R. Gáspár. 1995. Potassium channels regulate hypo-osmotic shock-induced motility of common carp (*Cyprinus carpio*) sperm. Aquaculture 129(1-4):123-128.

Krasznai, Z., T. Márián, H. Izumi, S. Damjanovich, L. Balkay, L. Trón, and M. Morisawa. 2000. Membrane hyperpolarization removes inactivation of Ca^{2+} channels, leading to Ca^{2+} influx and subsequent initiation of sperm motility in the common carp. Proceedings of the National Academy of Sciences of the United States of America 97:2052-2067.

Lahnsteiner, F., B. Berger, T. Weismann, and R. A. Patzner. 1996. Motility of spermatozoa of *Alburnus alburnus* (Cyprinidae) and its relationship to seminal plasma composition and sperm metabolism. Fish Physiology and Biochemistry 15:167-179.

Le, M. H., H. K. Lim, B. H. Min, M. S. Park, M. H. Son, J. U. Lee, and Y. J. Chang. 2011. Effects of varying dilutions, pH, temperature and cations on spermatozoa motility in fish *Larimichthys polyactis*. Journal of Environmental Biology 32(3):271-276.

Le, M. H., and H. Q. Pham. 2017. Sperm motilities in Waigieu seaperch, *Psammoperca waigiensis*: Effects of various dilutions, pH, temperature, osmolality, and cations. Journal of the World Aquaculture Society 48(3):435-443.

Levitan, D.R. 1995. The ecology of fertilization in free-spawning invertebrates. In: Ecology of Marine Invertebrate Larvae. McEdward, L.R. (ed). CRC Press, Boca Raton, FL, USA, pp. 123-156.

Mocanu, M. M., S. Gadgil, D. M. Yellon, and G. F. Baxter. 1999. Mibefradil, a T-type and L-type calcium channel blocker, limits infarct size through a glibenclamide-sensitive mechanism. Cardiovascular Drugs and Therapy 13(2):115–122.

Morisawa, M., 1985. Initiation mechanism of sperm motility at spawning in teleosts. Zoological Science 2:605-615.

Morisawa, M. 2008. Adaptation and strategy for fertilization in the sperm of teleost fish. Journal of Applied Ichthyology 24(4): 362-370.

Morisawa, M., M. Okuno, K. Suzuki, S. Morisawa, and K. Ishida. 1983a. Initiation of sperm motility in teleosts. Journal of Submicroscopic Cytology and Pathology 15(1):61-65.

Morisawa, M., Suzuki, K., 1980. Osmolality and potassium ion: their roles in initiation of sperm motility in teleosts. Science 210:1145-1147.

Morisawa, M., K. Suzuki, and S. Morisawa. 1983b. Effects of potassium and osmolality on spermatozoan motility of salmonid fishes. Journal of Experimental Biology 107:105-113.

Morisawa, M., K. Suzuki, H. Shimizu, S. Morisawa, and K. Yasuda. 1983c. Effects of osmolality and potassium on motility of spermatozoa from freshwater cyprinid fishes. Journal of Experimental Biology 107:95-103.

Nakajima, A., M. Morita, A. Takemura, S. Kamimura, and M. Okuno. 2005. Increase in intracellular pH induces phosphorylation of axonemal proteins for activation of flagellar motility in starfish sperm. Journal of Experimental Biology 208:4411-4418.

Naylor, R. L., R. J. Goldburg, J. H. Primavera, N. Kautsky, M. C. M. Beveridge, J. Clay, C. Folke, J. Lubchenco, H. Mooney, and M. Troell. 2000. Effect of aquaculture on world fish supplies. Nature 405:1017–1024.

Ozbay, G., B. Reckenbeil, F. Marenghi, and P. Erbland. 2017. Eastern oyster (*Crassostrea virginica*) aquaculture and diversity of associated species. In: Oysters: Biology, Consumption and Ecological Importance. Marine Biology. Nova Science Publishers, Incorporated, Hauppauge, NY, pp. 1-54.

Piferrer, F., A. Beaumont, J. C. Falguière, M. Flajšhans, P. Haffray, and L. Colombo. 2009. Polyploid fish and shellfish: Production, biology and applications to aquaculture for performance improvement and genetic containment. Aquaculture 293:125156.

Prytherch, H. F. 1928. Investigation of the physical conditions controlling spawning of oysters and the occurrence, distribution, and setting of oyster larvae in Milford Harbor, Connecticut. Bulletin of the Bureau of Fisheries 4:429-503.

Rurangwa, E., D. E. Kime, F. Ollevier, and J. P. Nash. 2004. The measurement of sperm motility and factors affecting sperm quality in cultured fish. Aquaculture 234(1-4):1-28.

Rurangwa, E., F. A. M. Volckaert, G. Huyskens, D. E. Kime, and F. Ollevier. 2001. Quality control of refrigerated and cryopreserved semen using computer-assisted sperm analysis (CASA), viable staining and standardized fertilization in African catfish (*Clarias gariepinus*). Theriogenology 55:751-769.

Shiba, K., T. Márián, Z. Krasznai, S. A. Baba, M. Morisawa, and M. Yoshida. 2006. Na^{+}/Ca^{2+} exchanger modulates the flagellar wave pattern for the regulation of motility activation and chemotaxis in the ascidian spermatozoa. Cell Motility and the Cytoskeleton 63:623-632.

Song, Y. P., M. Suquet, I. Quéau, and L. Lebrun. 2009. Setting of a procedure for experimental fertilisation of Pacific oyster (*Crassostrea gigas*) oocytes. Aquaculture 287(3-4):311-314.

Spilke, J., H. P. Piepho, and X. Hu. 2005. Analysis of unbalanced data by mixed linear models using the MIXED procedure of the SAS system. Journal of Agronomy and Crop Science 191:47-54.

Stoss, J. 1983. Fish gamete preservation and spermatozoan physiology. Fish Physiology 9:305-350.

Vignier, J., A. K. Volety, A. Rolton, R. Robert, and P. Soudant. 2017. Sensitivity of Eastern oyster (*Crassostrea virginica*) spermatozoa and oocytes to dispersed oil: Cellular responses and impacts on fertilization and embryogenesis. Environmental Pollution 225:270-282.

Vílchez, M. C., M. Morini, D. S. Peñaranda, V. Gallego, J. F. Asturiano, and L. Pérez. 2016. Sodium affects the sperm motility in the European eel. Comparative Biochemistry and Physiology -Part A: Molecular and Integrative Physiology 198:51-58.

Vines, C. A., K. Yoshida, F. J. Griffin, M. C. Pillai, M. Morisawa, R. Yanagimachi, and G. N. Cherr. 2002. Motility initiation in herring sperm is regulated by reverse sodium-calcium exchange. Proceedings of the National Academy of Sciences of the United States of

America 2006(30):1-14.

Wachten, D., J. F. Jikeli, and U. B. Kaupp. 2017. Sperm sensory signaling. Cold Spring Harbor Perspectives in Biology 147:dev181057.

Wallace, D.H. l 966. Oysters in the estuarine environment. A symposium of estuarine fisheries. American Fisheries Society, Special Publication 3:68-73.

Yang, H., E. Hu, R. Cuevas-uribe, J. Supan, X. Guo, and T. R. Tiersch. 2012. High-throughput sperm cryopreservation of eastern oyster *Crassostrea virginica*. Aquaculture 344-349:223-230.

Zilli, L., R. Schiavone, C. Storelli, and S. Vilella. 2008. Molecular Mechanisms Determining Sperm Motility Initiation in Two Sparids (*Sparus aurata* and *Lithognathus mormyrus*). Biology of Reproduction 79(2):356-366.

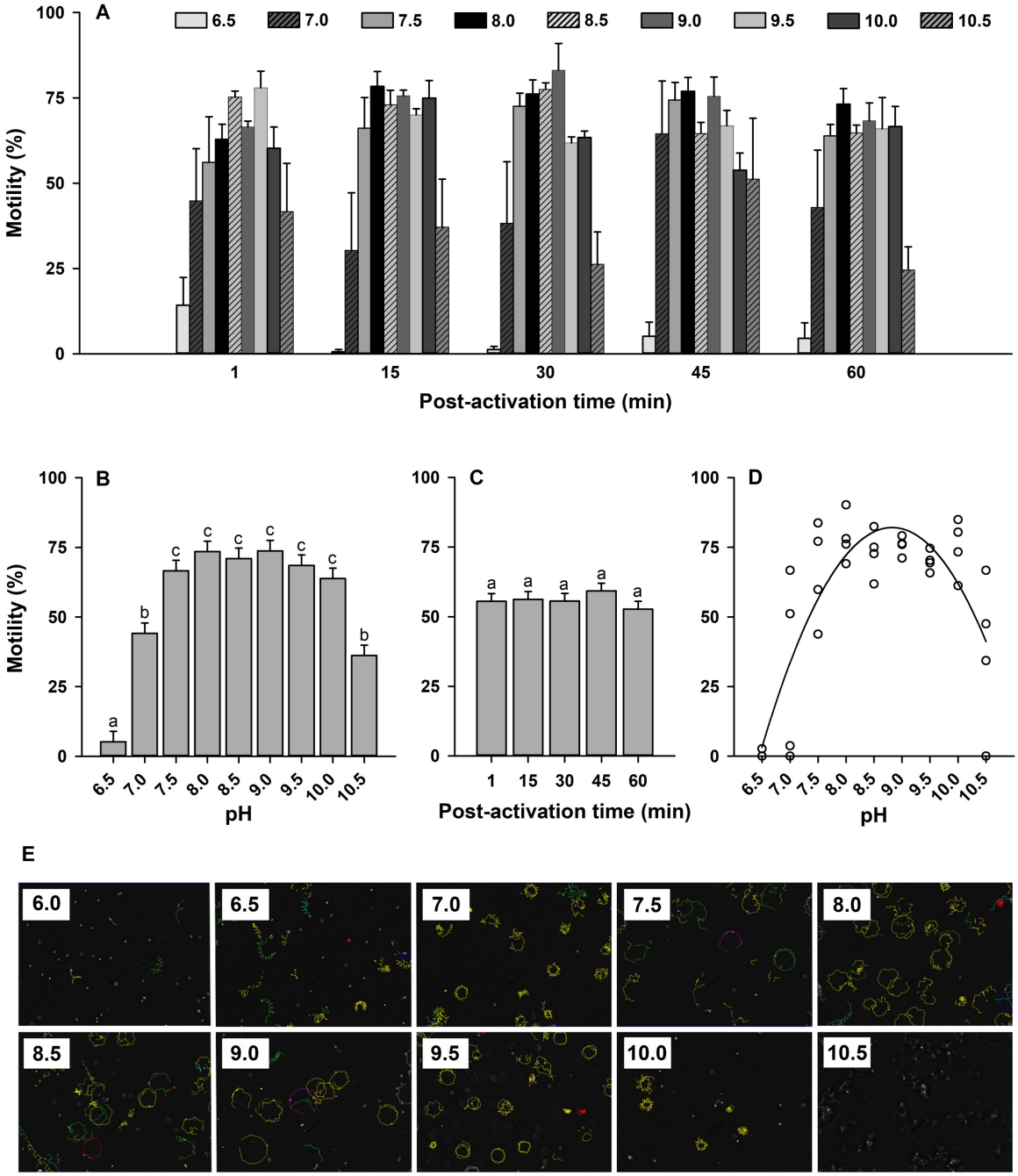

Figure 1.1 Effect of pH on sperm motility (%) in Eastern oyster, *Crassostrea virginica*. Sperm from four males were activated with artificial seawater (ASW) buffered to a pH of 6.5 to 10.5. Motility was estimated at 1, 15, 30, 45, and 60 min post-activation (A). Average motility (%) at each pH (B) and post-activation time (min) (C) is displayed. Sperm motility (%) of individual males at each pH is modeled by a second-order polynomial regression at 15 min post-activation (D). CASA images show sperm trajectories representing motility at each pH (E). Data were analyzed using a repeated measures factorial ANOVA model. Error bars represent least square means standard error. Treatments without a common superscript significantly differed ($P < 0.05$).

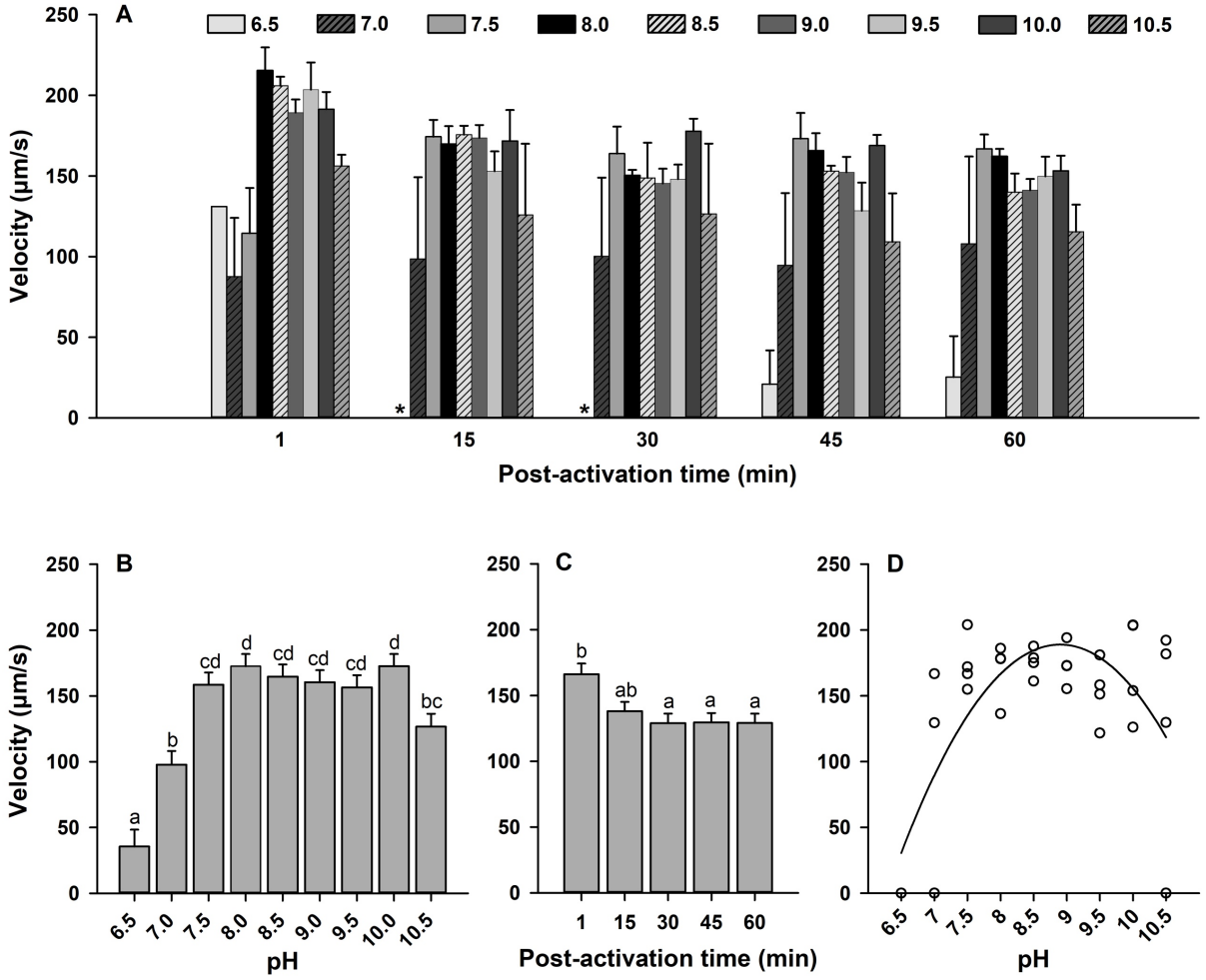

Figure 1.2 Effect of pH on sperm velocity (µm/s) in Eastern oyster, *Crassostrea virginica*. Sperm from four males were activated with artificial seawater (ASW) buffered to a pH of 6.5 to 10.5. Sperm velocity was estimated at 1, 15, 30, 45, and 60 min post-activation (A). Average velocity (µm/s) at each pH (B) and post-activation time (min) (C) is displayed. Sperm velocity (µm/s) of individual males at each pH is modeled by a second-order polynomial regression at 15 min post-activation (D). Data were analyzed using a repeated measures factorial ANOVA model. Error bars represent least square means standard error. Treatments without a common superscript significantly differed ($P < 0.05$). A velocity of 0 is indicated by *.

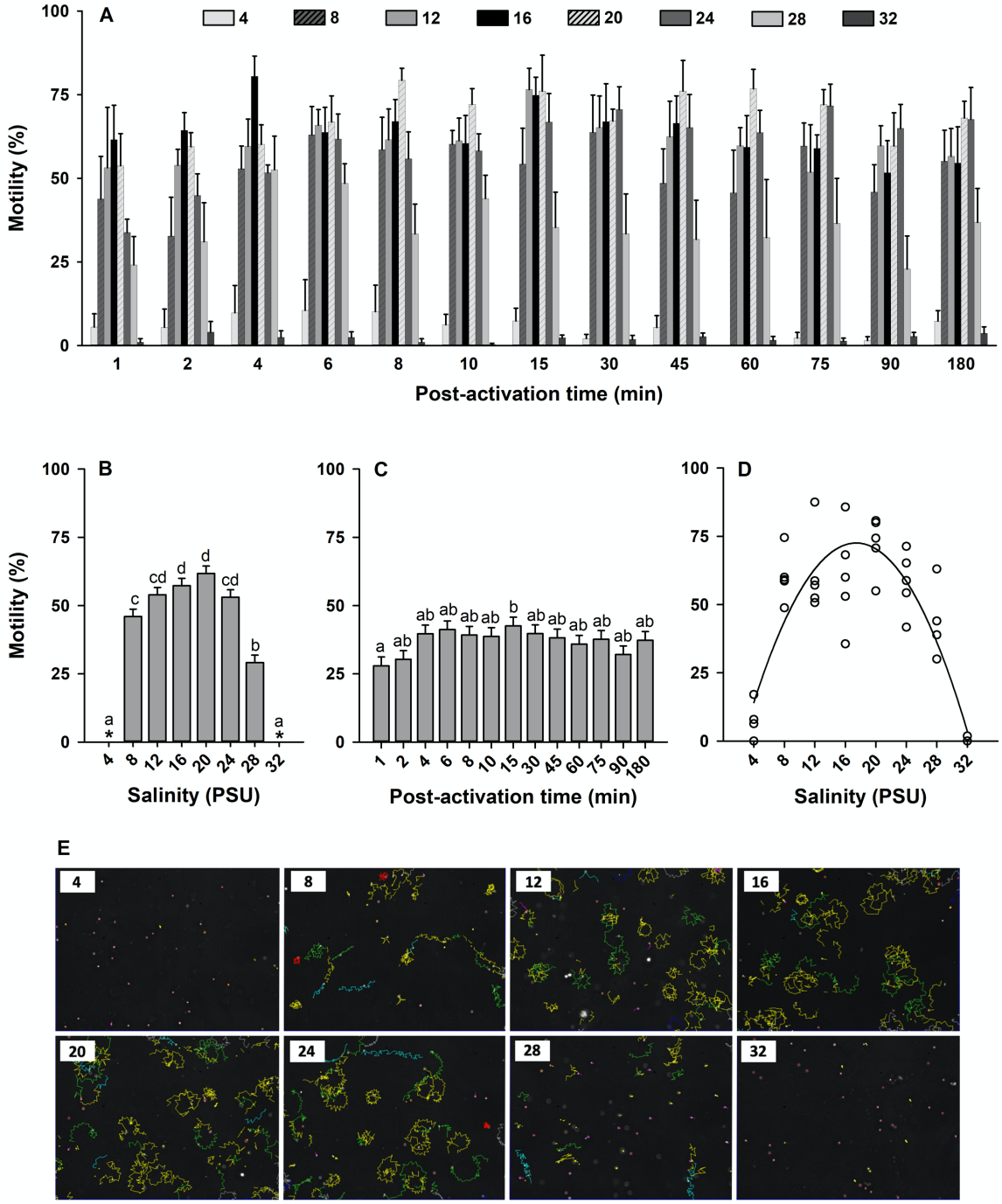

Figure 1.3 Effect of salinity on sperm motility (%) in Eastern oyster, *Crassostrea virginica*. Sperm from five males were activated with high salinity coastal seawater diluted to salinities of 4 to 32 PSU. Motility was estimated at 1 to 180 min post-activation (A). Average motility (%) at each salinity (B) and post-activation time (min) (C) is displayed. Sperm motility (%) of individual males at each salinity is modeled by a second-order polynomial regression at 15 min post-activation (D). CASA images show sperm trajectories representing motility at each salinity (E). Data were analyzed using a repeated measures factorial ANOVA model. Error bars represent least square means standard error. Treatments without a common superscript significantly differed ($P < 0.05$). A motility of 0 is indicated by *.

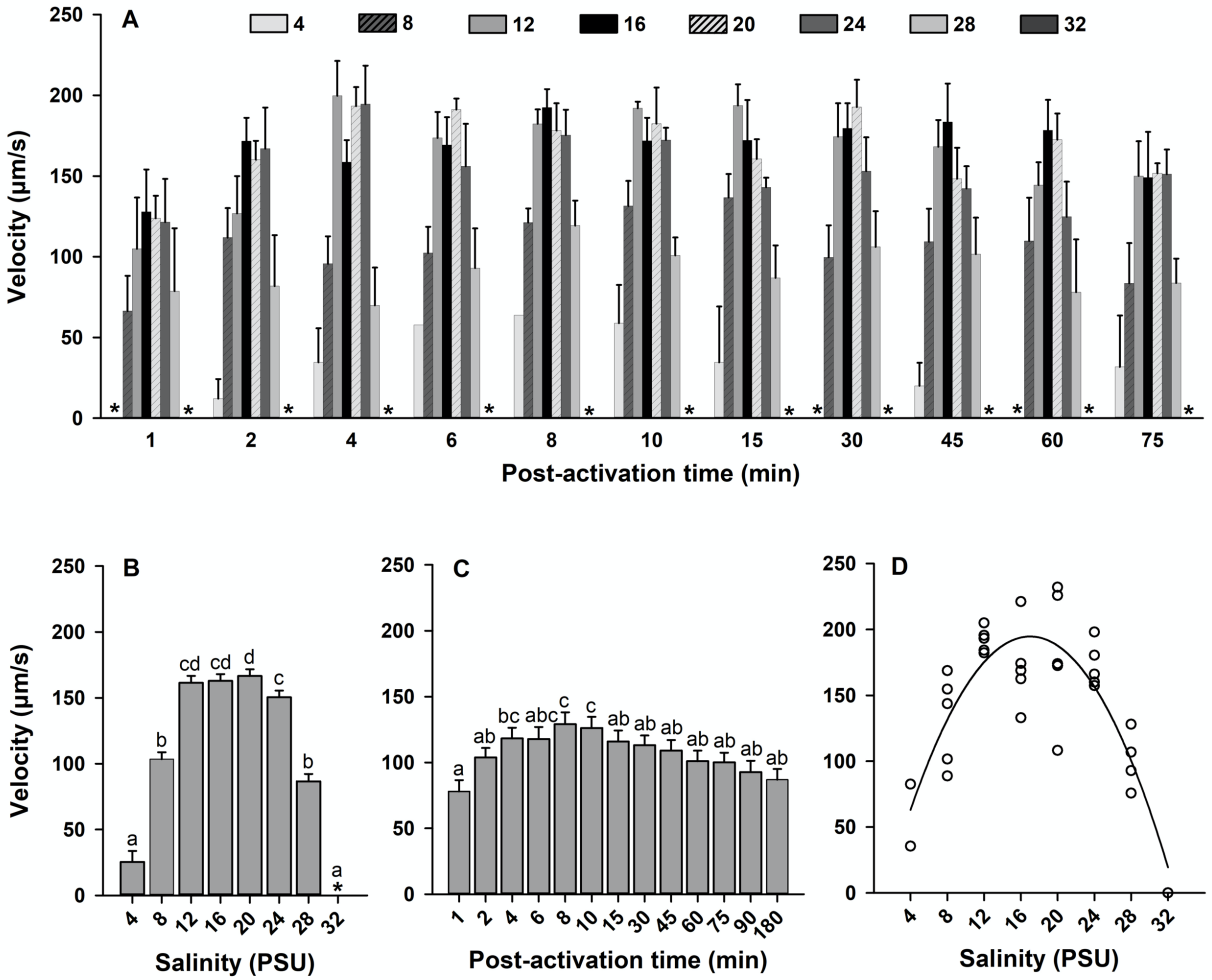

Figure 1.4 Effect of salinity on sperm velocity (µm/s) in Eastern oyster, *Crassostrea virginica*. Sperm from five males were activated with high salinity coastal seawater diluted to salinities of 4 to 32 PSU. Sperm velocity was measured at 1 to 180 min post-activation (A). Average velocity (µm/s) at each salinity (B) and post-activation time (min) (C) is displayed. Sperm velocity (µm/s) of individual males at each salinity is modeled by a second-order polynomial regression at 15 min post-activation (D). Data were analyzed using a repeated measures factorial ANOVA model. Error bars represent least square means standard error. Treatments without a common superscript significantly differed ($P < 0.05$). A velocity of 0 is indicated by *.

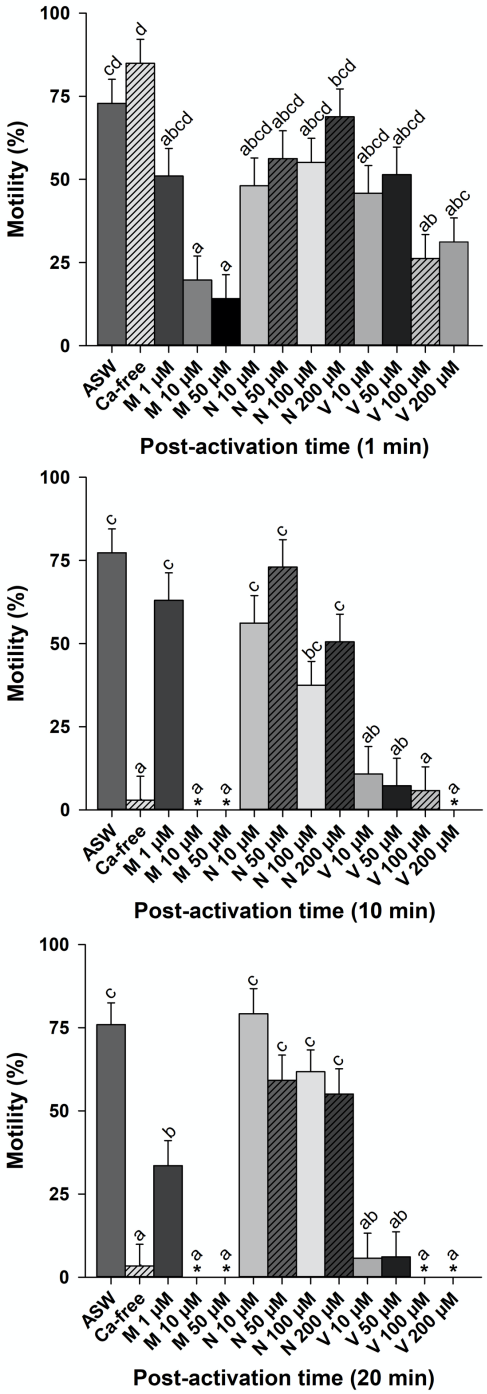

Figure 1.5 Effect of Ca^{2+}-free artificial seawater (ASW) and Ca^{2+} channel blockers on sperm motility (%) in Eastern oyster*, Crassostrea virginica*. Sperm from four males were activated with ASW, Ca^{2+}-free ASW, and channel blockers, mibefradil (1, 5, 10, and 50 µM), nifedipine (10, 50, 100, and 200 µM), and verapamil (10, 50, 100, and 200 µM). Motility was measured at 1, 10, and 20 min post-activation. Data were analyzed using a repeated measures factorial ANOVA model. Error bars represent least square means standard error. Treatments without a common superscript significantly differed ($P < 0.05$). A motility of 0 is indicated by *.

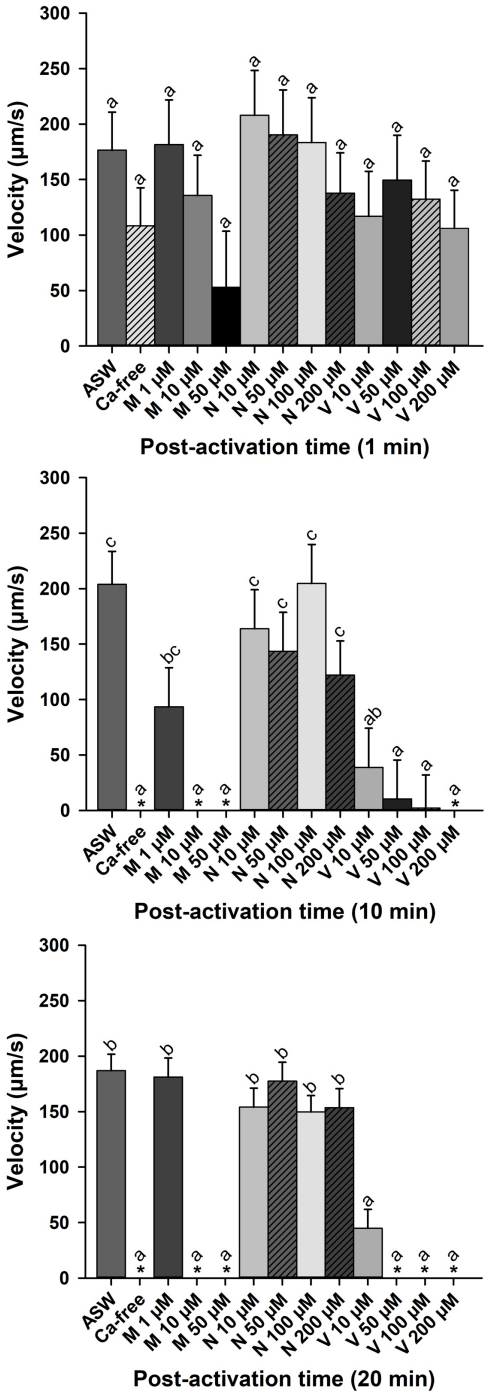

Figure 1.6 Effect of Ca^{2+}-free artificial seawater (ASW) and Ca^{2+} channel blockers on sperm velocity (µm/s) in Eastern oyster*, Crassostrea virginica*. Sperm from four males were activated with ASW, Ca^{2+}-free ASW, and channel blockers, mibefradil (1, 5, 10, and 50 µM), nifedipine (10, 50, 100, and 200 µM), and verapamil (10, 50, 100, and 200 µM). Sperm velocity was measured at 1, 10, and 20 min post-activation. Data were analyzed using a repeated measures factorial ANOVA model. Error bars represent least square means standard error. Treatments without a common superscript significantly differed ($P < 0.05$). A velocity of 0 is indicated by *.

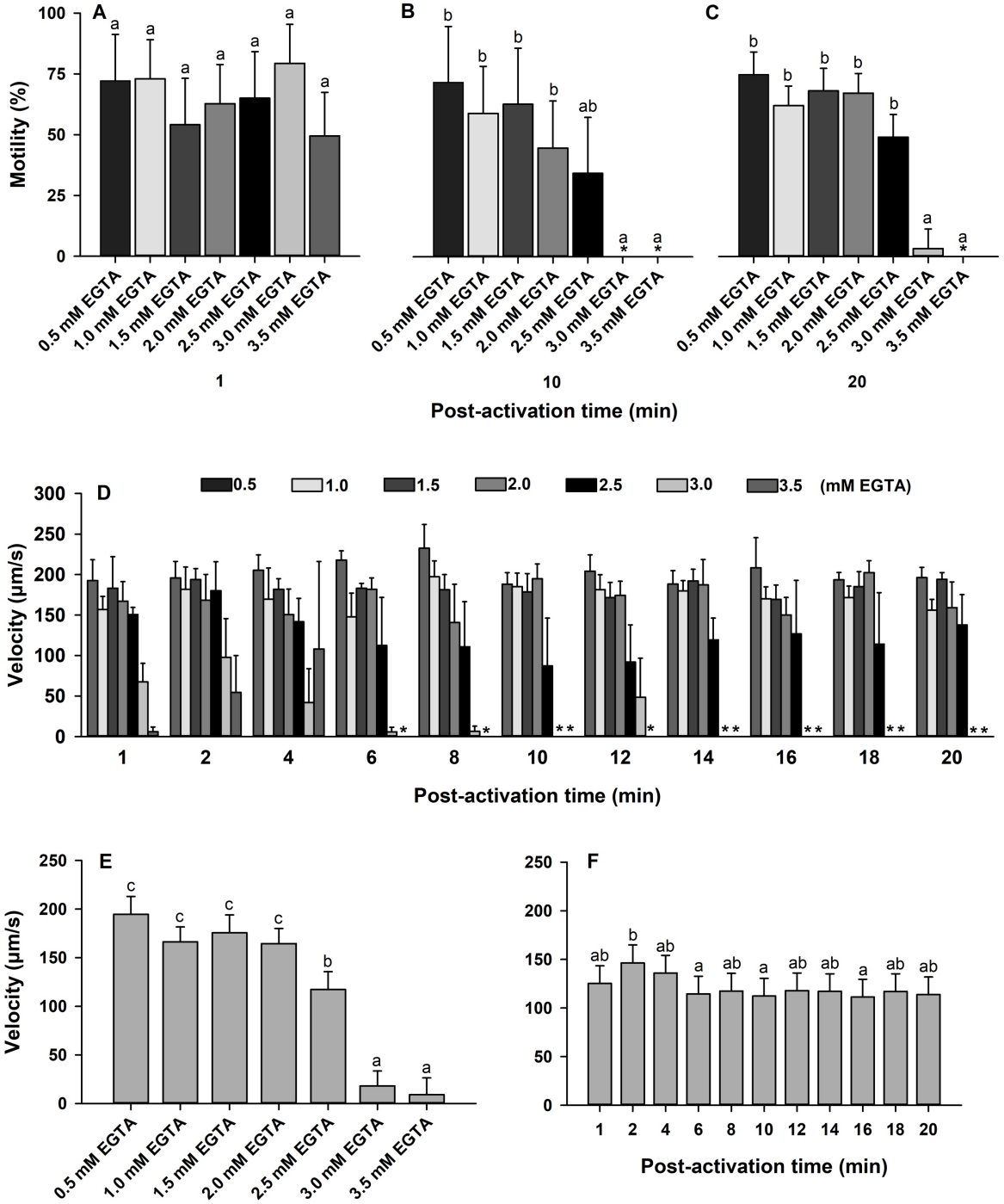

Figure 1.7 Effect of EGTA on sperm motility (%) and velocity (µm/s) in Eastern oyster, *Crassostrea virginica*. Sperm from four males were activated with EGTA (0.5 to 3.5 mM) and analyzed at 1 to 20 min post-activation with motility (%) (ABC) and velocity (µm/s) (D) displayed. Average velocity (µm/s) at each EGTA concentration (E) and post-activation time (min) (F) is displayed. Data were analyzed using a repeated measures factorial ANOVA model. Error bars represent least square means standard error. Treatments without a common superscript significantly differed ($P < 0.05$). Motility and velocity of 0 are indicated by *.

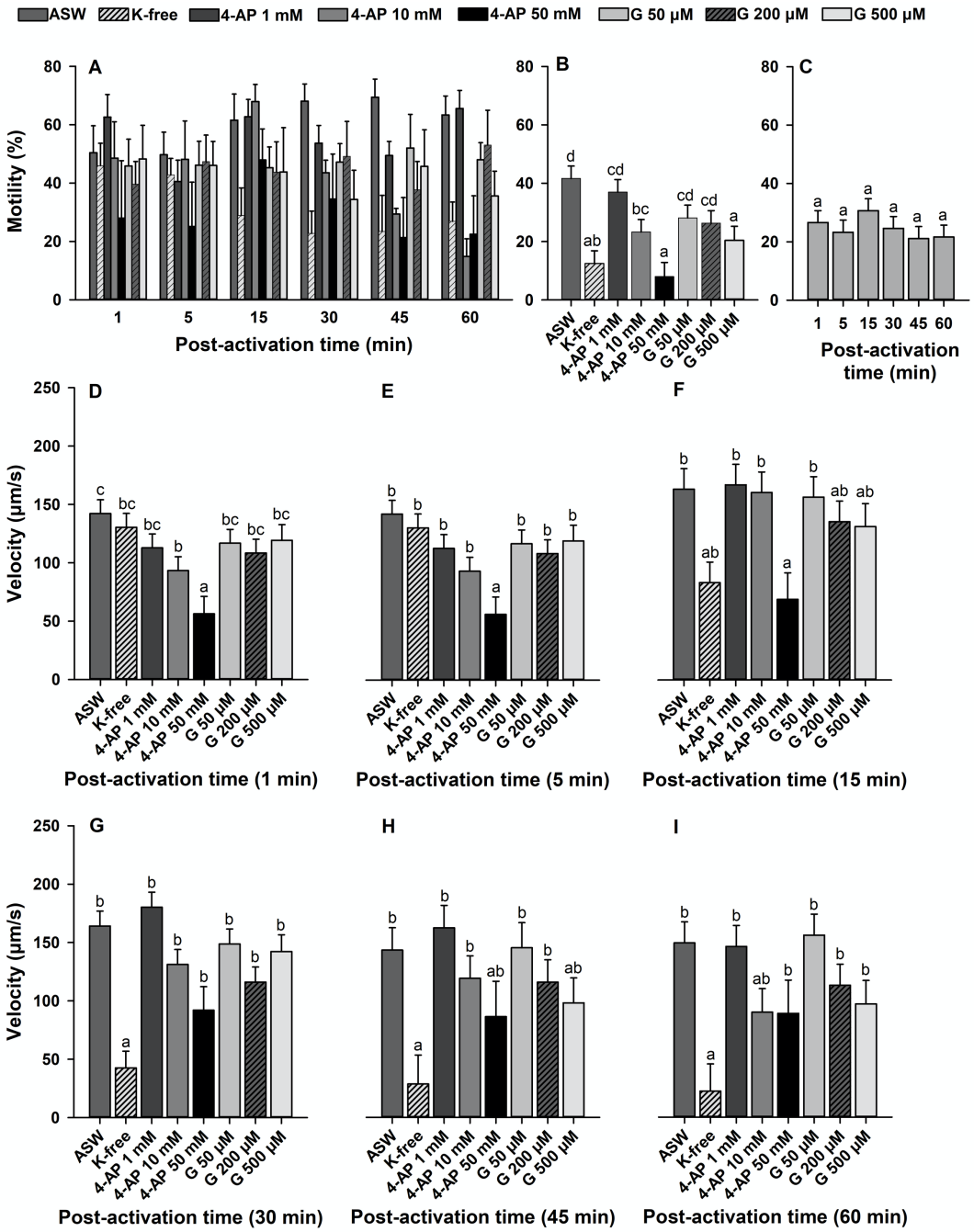

Figure 1.8 Effect of K^+-free artificial seawater (ASW) and K^+ channel blockers on sperm motility (%) and velocity (µm/s) in Eastern oyster, *Crassostrea virginica*. Sperm from five males were activated with ASW, K^+-free ASW, and channel blockers, 4-aminopyridine (4-AP) (1, 10, 50 mM) and glybenclamide (50, 200, 500 µM). Motility was measured at 1 to 60 min post-activation (A). Motility (%) with each activating solution (B) and post-activation time (min) (C) is displayed. Velocity (µm/s) with each activating solution at 1 to 60 min post-activation time (D) is displayed. Data were analyzed using a repeated measures factorial ANOVA model. Error bars represent least square means standard error. Treatments without a common superscript significantly differed ($P < 0.05$).

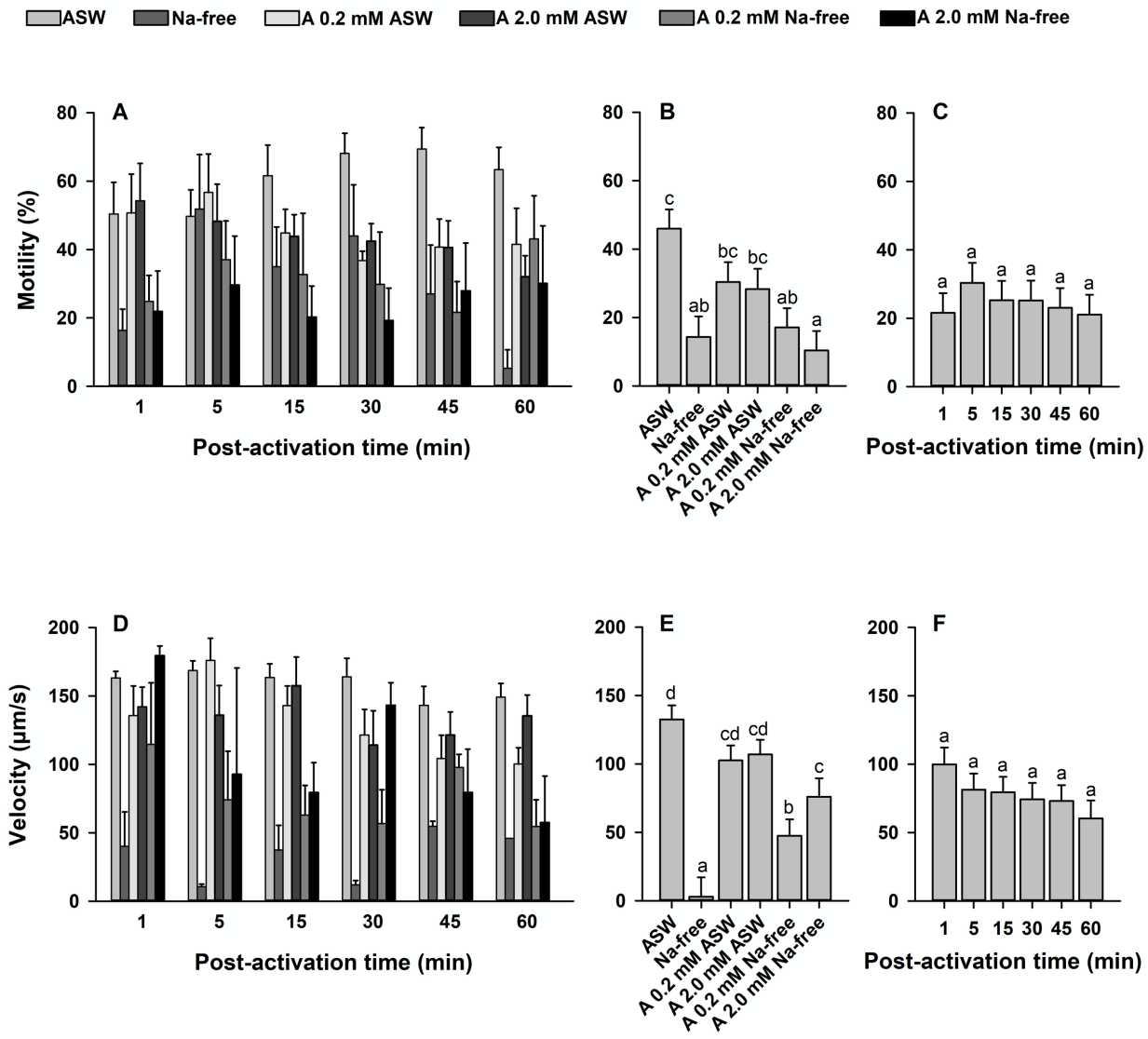

Figure 1.9 Effect of Na^+-free artificial seawater (ASW) and Na^+ channel blockers on sperm motility (%) and velocity (µm/s) in Eastern oyster, *Crassostrea virginica*. Sperm from five males were activated with ASW, Na^+-free ASW, and the channel blocker, amiloride (0.2 and 2.0 mM), added to ASW and Na^+-free ASW. Motility and sperm velocity were measured at 1 to 60 min post-activation (AD). Motility (%) with each activating solution (B) and post-activation time (min) (C) is displayed. Velocity (µm/s) with each activating solution (E) and post-activation time (min) (F) is displayed. Data were analyzed using a repeated measures factorial ANOVA model. Error bars represent least square means standard error. Treatments without a common superscript significantly differed ($P < 0.05$).

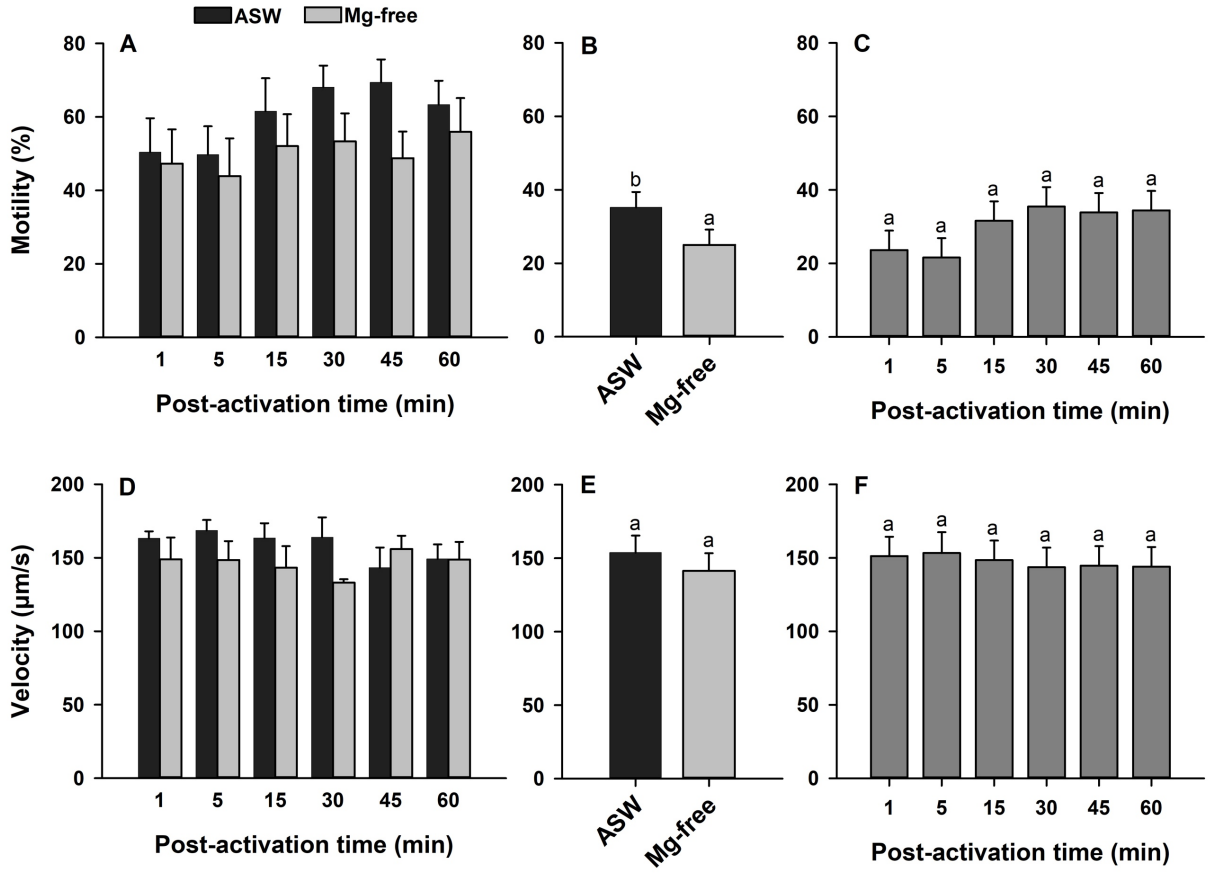

Figure 1.10 Effect of Mg^{2+}-free artificial seawater (ASW) on sperm motility (%) and velocity (µm/s) in Eastern oyster, *Crassostrea virginica*. Sperm from five males were activated with ASW, Mg^{2+}-free ASW. Motility and sperm velocity were measured at 1 to 60 min post-activation (AD). Motility (%) with each activating solution (B) and post-activation time (min) (C) is displayed. Velocity (µm/s) with each activating solution (E) and post-activation time (min) (F) is displayed. Data were analyzed using a repeated measures factorial ANOVA model. Error bars represent least square means standard error. Treatments without a common superscript significantly differed ($P < 0.05$).

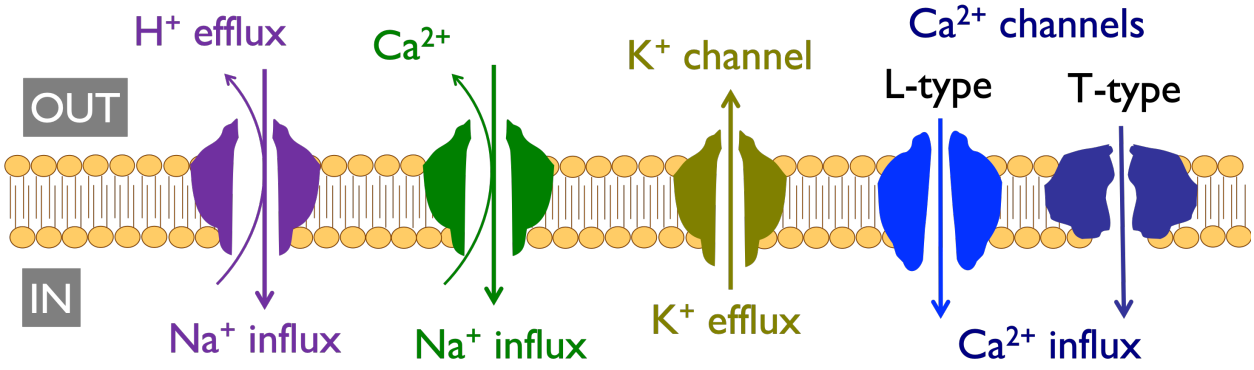

Figure 1.11 Signaling pathways and ion channels in the sperm membrane responsible for motility initiation in bivalves. This figure is modified from Boulais et al. (2019). When sperm is discharged into seawater, motility initiation occurs from a Na^+-dependent alkalization of internal pH facilitated through the exchange of Na^+ and H^+. Moreover, K^+ efflux through voltage-dependent K^+ channels generates hyperpolarization of sperm membrane potential. Under alkaline conditions, voltage-dependent Ca^{2+} channels open, allowing for Ca^{2+} influx which triggers Ca^{2+}/calmodulin-dependent flagellar beating.

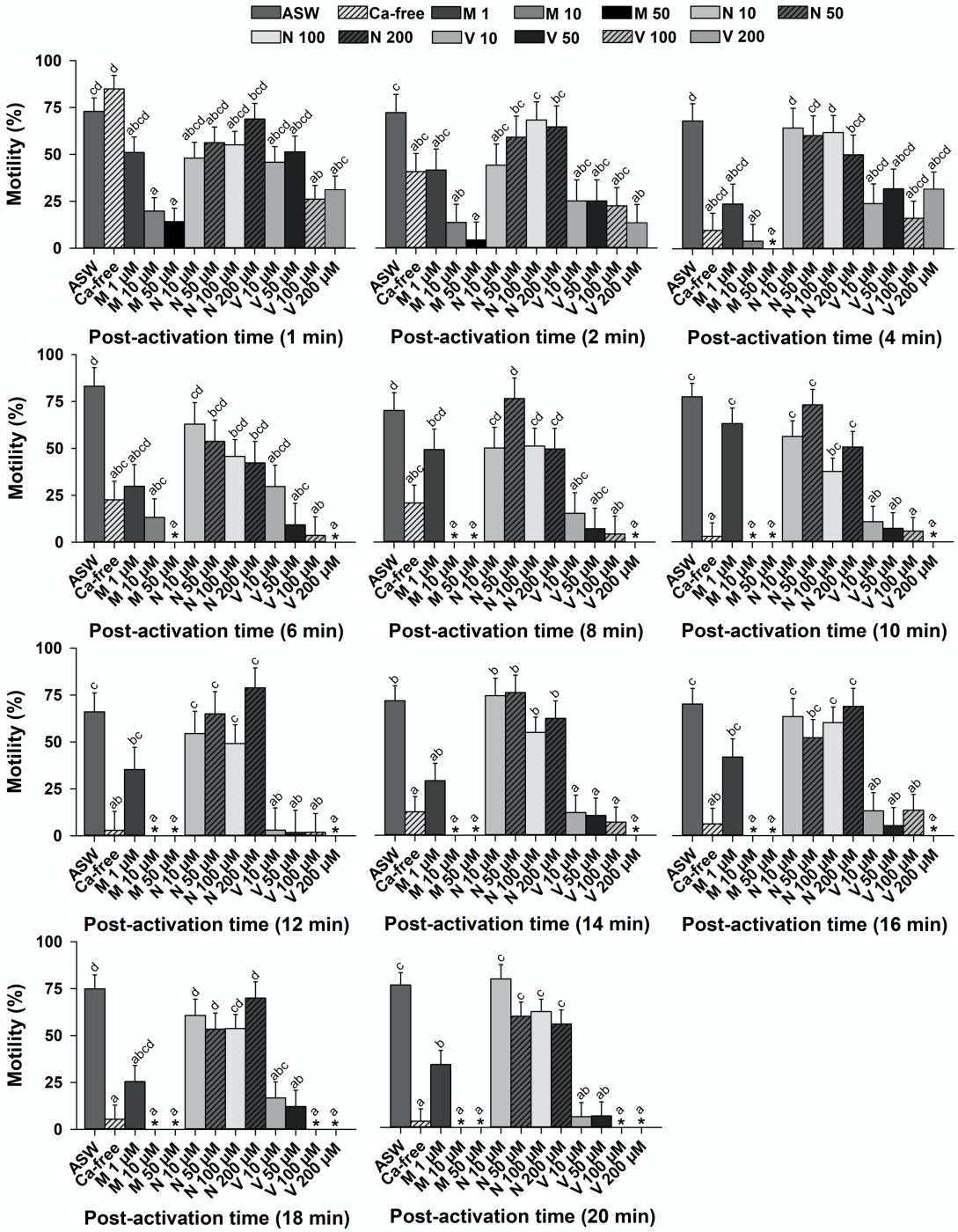

Supplementary Figure 1.1 Effect of Ca^{2+}-free artificial seawater (ASW) and Ca^{2+} channel blockers on sperm motility (%) in Eastern oyster, *Crassostrea virginica*. Sperm from four males were activated with ASW, Ca^{2+}-free ASW, and channel blockers, mibefradil (1, 5, 10, and 50 μM), nifedipine (10, 50, 100, and 200 μM), and verapamil (10, 50, 100, and 200 μM). Motility was measured at 1 to 20 min post-activation. Data were analyzed using a repeated measures factorial ANOVA model. Error bars represent least square means standard error. Treatments without a common superscript significantly differed ($P < 0.05$). Motility of 0 is indicated by *.

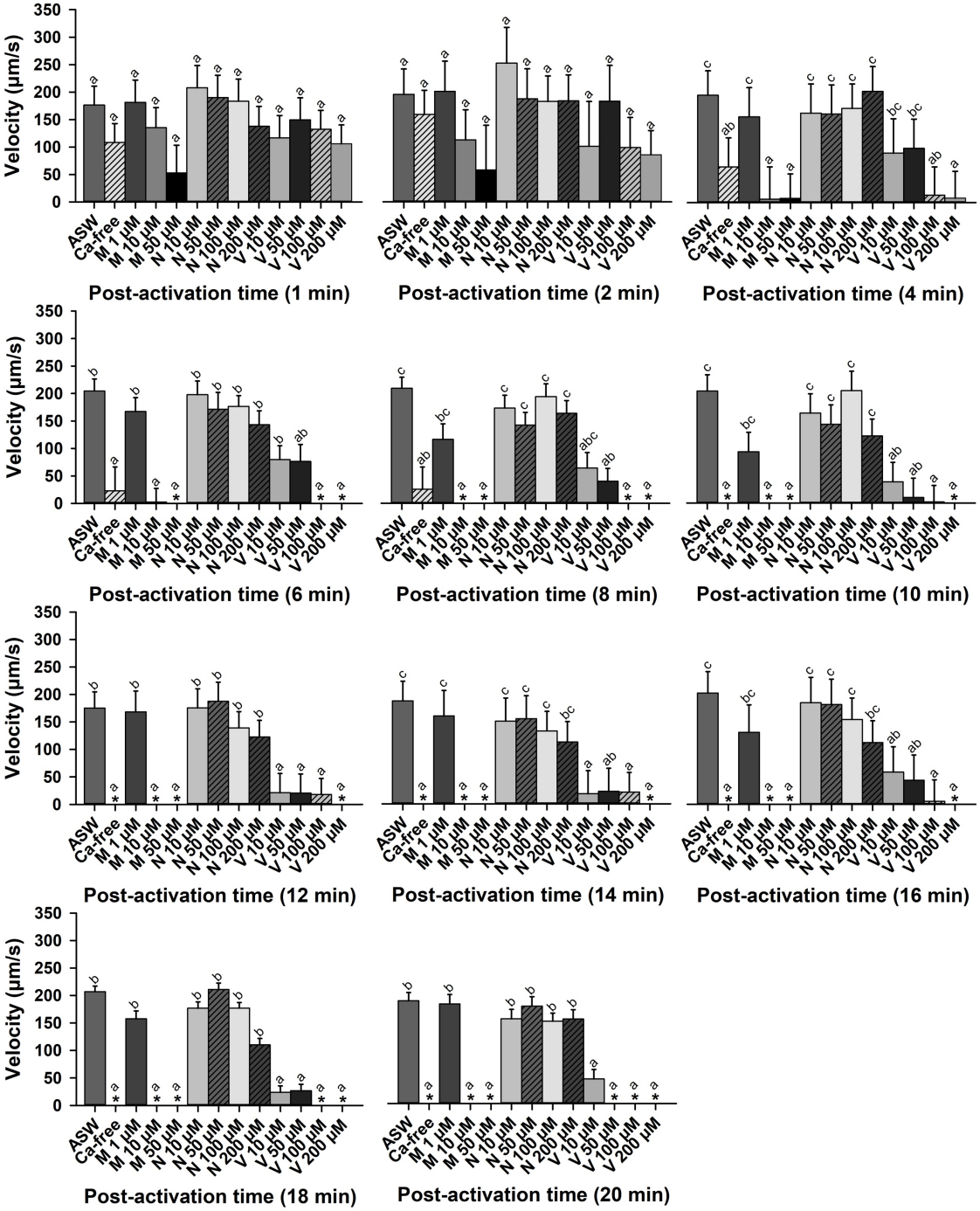

Supplementary Figure 1.2 Effect of Ca^{2+}-free artificial seawater (ASW) and Ca^{2+} channel blockers on sperm velocity (µm/s) in Eastern oyster, *Crassostrea virginica*. Sperm from four males were activated with ASW, Ca^{2+}-free ASW, and channel blockers, mibefradil (1, 5, 10, and 50 µM), nifedipine (10, 50, 100, and 200 µM), and verapamil (10, 50, 100, and 200 µM). Sperm velocity was measured at 1 to 20 min post-activation. Data were analyzed using a repeated measures factorial ANOVA model. Error bars represent least square means standard error. Treatments without a common superscript significantly differed ($P < 0.05$). Velocity of 0 is indicated by *.

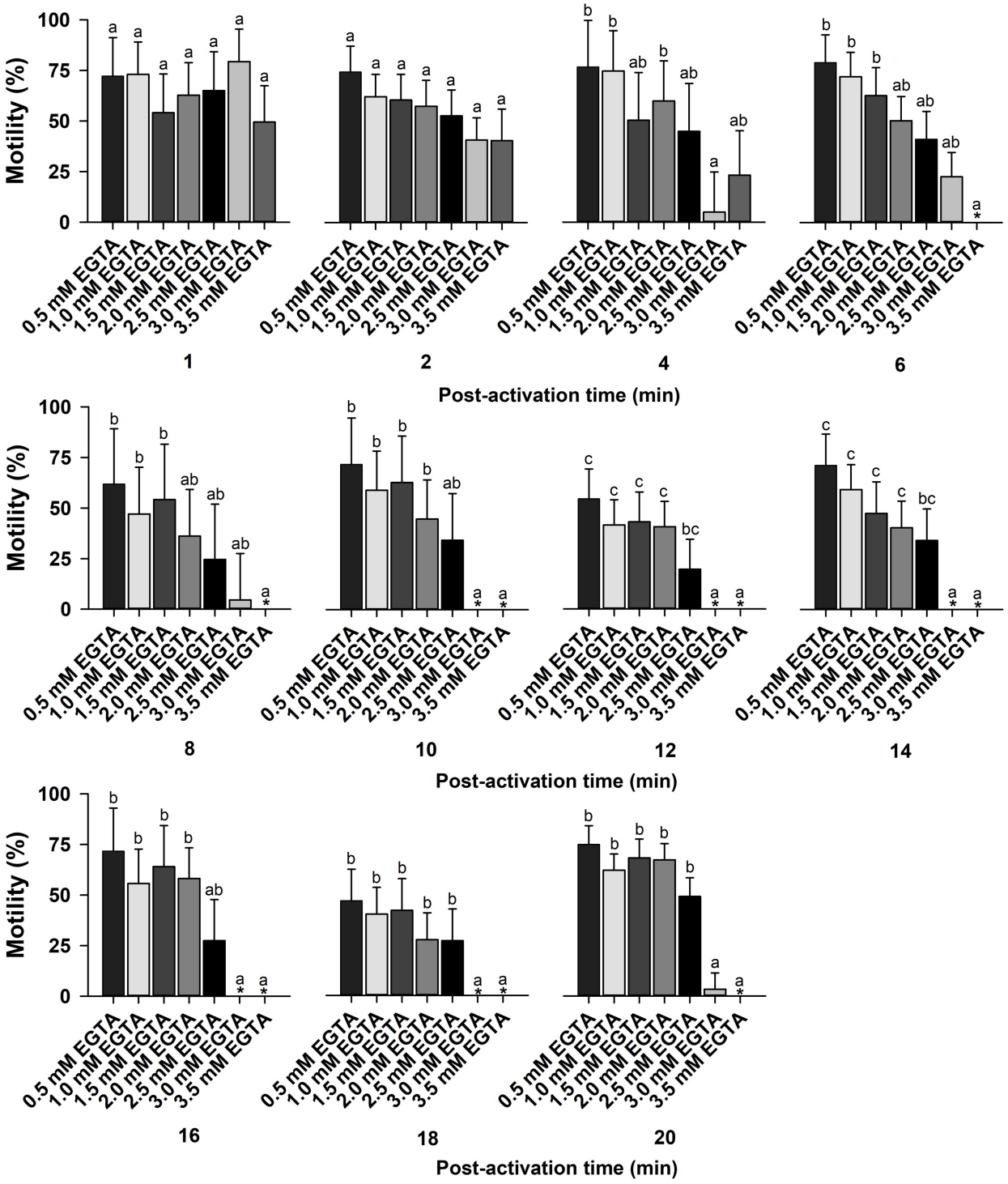

Supplementary Figure 1.3 Effect of EGTA on sperm motility (%) in Eastern oyster, *Crassostrea virginica*. Sperm from four males were activated with EGTA (0.5 to 3.5 mM). Motility was measured at 1 to 20 min post-activation. Data were analyzed using a repeated measures factorial ANOVA model. Error bars represent least square means standard error. Treatments without a common superscript significantly differed ($P < 0.05$). Motility of 0 is indicated by *.

Table 1.1 pH and osmolality (mOsmol/kg) of Eastern oyster (n = 5), *Crassostrea virginica*, testicular fluid.

Oyster	pH	Osmolality (mOsmol/kg)
1	5.99	554.33
2	5.81	600.67
3	5.77	476.33
4	5.84	682.67
5	5.97	534.00

Table 1.2 Morphometrics including length (mm), width (mm), height (mm), weight (g), and sperm density (cells/mL) of individual Eastern oyster, *Crassostrea virginica*, males used to study physiological mechanisms regulating sperm motility initiation.

	Oyster	Shell length (mm)	Shell width (mm)	Shell height (mm)	Total weight (g)	Sperm density (cells/mL)
Exp. 1.1. pH	1	50.10	23.20	69.40	48.16	9.40E+08
	2	52.60	26.70	65.50	49.15	6.23E+08
	3	45.00	26.20	67.50	48.19	9.53E+08
	4	49.60	26.10	66.80	52.02	1.29E+09
Exp. 1.2. Salinity	1	55.76	36.10	96.65	128.03	3.51E+09
	2	58.51	32.40	106.66	140.20	6.03E+09
	3	59.20	34.90	89.48	115.71	2.76E+09
	4	57.07	27.14	108.91	129.10	4.26E+09
	5	57.97	37.08	84.30	90.18	2.34E+09
Exp. 1.3. Ca^{2+}	1	66.09	36.45	92.73	135.05	5.12E+10
	2	60.85	41.64	88.06	146.87	5.53E+10
	3	56.41	33.90	94.76	103.90	2.81E+10
	4	60.19	38.25	95.46	146.53	3.92E+10
Exp. 1.3. K^+, Na^+, & Mg^{2+}	1	67.20	34.50	95.40	116.85	1.60E+09
	2	65.20	36.70	113.60	143.42	1.89E+10
	3	67.80	45.50	100.40	145.71	4.98E+09
	4	57.20	39.30	97.20	127.26	1.72E+10
	5	63.10	42.30	92.70	146.14	4.46E+09

Table 1.3 Salinities and corresponding osmolalities (mOsmol/kg) for the Eastern oyster, *Crassostrea virginica* sperm activation solutions used in Experiment 2 (*Effect of Salinity*).

Salinity PSU	**Osmolality (mOsmol/kg)**
4	32.67
8	85.33
12	241.33
16	338.33
20	447.33
24	527.67
28	719.00
32	739.00

Table 1.4 Sperm activity parameters of the Eastern oyster, *Crassostrea virginica*, from the pH and salinity experiments modeled by second-order polynomial regressions. For each time, the equation of the line, R^2 value, and absolute maximum or peak (vertex) are shown in columns for both motility and velocity. Significant values are denoted by ***P < 0.0001 and **P < 0.01.

	Time (min)	Motility (%)			Velocity (μm/s)		
		Equation	R^2	Vertex	Equation	R^2	Vertex
pH	1	$y = 188.84x - 758.02 - 10.71x^2$	0.54***	8.82	$y = 391.35x - 1575.18 - 21.52x^2$	0.46**	9.09
	15	$y = 257.61x - 1054.62 - 14.60x^2$	0.70***	8.83	$y = 489.72x - 1990.35 - 27.51x^2$	0.53***	8.90
	30	$y = 288.71x - 1166.46 - 16.67x^2$	0.75***	8.66	$y = 340.26x - 1369.31 - 18.82x^2$	0.31**	9.04
	45	$y = 196.31x - 775.53 - 11.28x^2$	0.46***	8.70	$y = 397.62x - 1585.12 - 22.52x^2$	0.44***	8.83
	60	$y = 237.22x - 953.99 - 13.66x^2$	0.65***	8.68	$y = 366.71x - 1458.62 - 20.70x^2$	0.48***	8.86
Salinity PSU	1	$y = 8.92x - 17.63 - 0.26x^2$	0.48***	16.83	$y = 23.83x - 85.50 - 0.65x^2$	0.44***	18.32
	2	$y = 10.41x - 30.61 - 0.29x^2$	0.68***	17.74	$y = 29.45x - 88.51 - 0.83x^2$	0.65***	17.84
	4	$y = 10.92x - 23.58 - 0.31x^2$	0.68***	17.54	$y = 34.43x - 99.05 - 0.99x^2$	0.63***	17.44
	6	$y = 10.76x - 19.19 - 0.31x^2$	0.67***	17.34	$y = 29.50x - 70.20 - 0.84x^2$	0.58***	17.48
	8	$y = 11.66x - 25.27 - 0.34x^2$	0.70***	17.14	$y = 27.42x - 43.02 - 0.78x^2$	0.68***	17.55
	10	$y = 11.31x - 25.94 - 0.32x^2$	0.77***	17.42	$y = 26.49x - 30.48 - 0.78x^2$	0.69***	17.00
	15	$y = 13.28x - 34.02 - 0.38x^2$	0.75***	17.39	$y = 25.84x - 27.77 - 0.78x^2$	0.63***	16.50
	30	$y = 12.36x - 31.36 - 0.35x^2$	0.66***	17.42	$y = 34.68x - 115.80 - 0.97x^2$	0.75***	17.92
	45	$y = 12.58x - 36.16 - 0.36x^2$	0.68***	17.64	$y = 28.74x - 73.09 - 0.82x^2$	0.65***	17.51
	60	$y = 12.80x - 42.07 - 0.36x^2$	0.69***	17.91	$y = 32.22x - 105.68 - 0.92x^2$	0.71***	17.51
	75	$y = 11.95x - 33.72 - 0.34x^2$	0.63***	17.78	$y = 26.17x - 69.62 - 0.74x^2$	0.59***	17.73
	90	$y = 11.07x - 32.23 - 0.31x^2$	0.65***	17.64	$y = 30.67x - 108.52 - 0.86x^2$	0.51***	17.82
	180	$y = 10.72x - 25.36 - 0.30x^2$	0.62***	17.65	$y = 23.54x - 56.70 - 0.69x^2$	0.57***	17.10

Chapter 2

Quantifying sperm concentration and morphology for two species of unionid mussels

Nichols, Z.G., Dalal, V.B., Stoeckel, J.A., Wayman, W.R., Miller M., and Butts, I.A.E. Quantifying sperm concentration and morphology for two species of unionid mussels. To be submitted to *Animal Reproduction Science in April 2020*

Abstract

Freshwater unionid mussel diversity is declining, as more species are becoming extirpated or extinct at an alarming rate. While little can be done to bring back lost species, there is an opportunity to work on securing the fate of others that are threatened or endangered. This can be facilitated through gene banking and assisted reproduction to propagate these imperiled species. Unfortunately, limited information is available on freshwater mussel reproduction, especially as it relates to paternal (sperm) impacts. Thus, our objectives were to (i) quantify seasonal patterns in sperm concentration and morphology for two unionid mussels, *Ligumia subrostrata* and *Lampsilis straminea* (ii) identify and measure intraspecific heterogeneity for sperm morphometry traits, and (iii) develop an efficient method to quantify sperm concentration using a microspectrophotometer (NanoDrop®). Both freshwater mussel species were held separately in two ponds in fifteen ~1' diameter mesh cages where temperature at the sediment-water interface was recorded with HOBO temperature loggers. Starting on 29 August 2018, male mussels (n = 5 for each species) were sampled every two weeks. Using a small pipette tip, sperm were collected directly from the gonad. Sperm concentration was determined for each male using a hemocytometer and a NanoDrop® at 350, 600, and 700 nm. Sperm were fixed in 2.5% glutaraldehyde and examined using scanning electron microscopy (SEM). Sperm concentration for *L. subrostrata* ranged from 1.1×10^9 to 19.60×10^9 cells/mL with highest production from 26 September to 7 November. For *L. straminea* sperm concentration peaked (20.0×10^9 cells/mL) on 13 September and declined thereafter. Sperm were uniflagellated and SEM results for *L. subrostrata* and *L. straminea* showed mean head length and width were 3.38 ± 0.05 μm and 1.61 ± 0.01 μm and 3.37 ± 0.04 μm and 1.61 ± 0.01 μm, respectively. In regard to male heterogeneity,

both species displayed significant variation in total sperm head width and length among individual males and revealed positive correlations between sperm head length and width. Additionally, *L. subrostrata* males had high variation between individuals for flagella length and total length. Finally, there was a positive relationship between hemocytometer counts and NanoDrop absorbance for both species ($R^2 \geq 0.85$). Together, these results provide baseline data to better understand sperm biology, fertilization dynamics, and cryopreservation conditions for freshwater mussel species.

2.1 Introduction

The Southeastern United States is a global hotspot for freshwater unionid mussel biodiversity with approximately 278 species (Graf and Cummings 2007), where Alabama is home to over 175 species (Benz and Collins 2004). Freshwater mussels are considered keystone species and provide many ecological services such as biofiltration (Vaughn et al. 2008), stabilization of streambeds (Vaughn and Hakenkamp 2001), and serve as sentinels of environmental change (Vaughn 2017). Unfortunately, freshwater mussels represent one of the most imperiled group of organisms with the highest extinction rate in the world (Williams et al. 1993, Bogan 1993; Benz and Collins 2004; Haag and Williams 2014). The decline of this fauna is due to poor water quality (Downing et al. 2010), impoundments of rivers (Layzer et al. 1993; Vaughn and Taylor 1999; Watters 1999), and climate change (Haag and Warren 2008, Karl et al. 2009, Gough et al. 2012). Propagation through assisted reproduction may be a viable way to restore freshwater mussel species on the verge of extinction, a technique that is considered to be one of the greatest achievements towards freshwater mussel conservation (Haag and Williams 2014).

Freshwater mussels (order Unionida) reproduce by spermcasting, where males expel aggregates of sperm called spermatozeugmata into the water column and females passively acquire the sperm bundles during filter feeding (McMahon and Bogan 2001; Bishop and Pemberton, 2006). Upon fertilization, embryos develop into larvae, or glochidia, which are brooded in the gills of the female (Mackie 1984). Mature glochidia are obligate parasites and usually rely on a fish host (Haag and Warren 1997; Watters and O'Dee 1998; O'Brien and Brim-Box 1999), where they parasitize the gills or fins, undergo metamorphosis, and settle to the

stream bottom as free-living juvenile mussels (Arey 1932; Kat 1984). Freshwater mussels exhibit intricate reproductive strategies and life histories, and many features regarding basic sperm biology have yet to be investigated.

Sperm travels from the gonad, through the genital duct, and to the genital pore where it is then expelled from the excurrent siphon (Matteson 1948; Ram et al. 1996), and formation of spermatozeugmata occur around the time of release into the aquatic environment (Lynn 1994; Ishibashi et al. 2000). Spermatozeugmata consist of an acellular sphere less than 100 μm in diameter, into which thousands of sperm imbed their heads with tails extended around the sphere (Lynn 1994; Waller and Lasee 1997; Barnhart and Roberts 1997). While loose sperm collected from the gonad loses motility after a few minutes, sperm embedded into the spermatozeugmata can remain viable and are able to become motile 48 to 72 hours after release into water (Ishibashi et al. 2000). It is suggested that these sperm spheres function as a means of transportation over long distances and to increase fertilization success.

Freshwater mussels, along with most species in the class Bivalvia, have sperm of a primitive type, characterized by their small size, a short midpiece, 4 or 5 mitochondria, typical 9+2 axoneme, and a long flagellum (Franzén 1983; Hodgson and Bernard 1986; Healy et al. 2008). Additionally, freshwater mussel sperm are uniflagellate and typically lack an acrosome (Waller and Lasee 1997). Bivalve sperm structures that generally have the least variation are the flagella, centrioles, and mitochondria (Popham, 1979), while the nuclei and acrosome show great morphological diversity (Franzén, 1983; Eckelbarger and Davis, 1996; Erkan and Sousa, 2002).

Seasonal changes can affect sperm quantity and quality throughout the spawning process. Sperm ageing or sperm senescence is well documented in fish species (Rurangwa et al. 2004; Alavi et al. 2008; Cabrita et al. 2009). Sperm production and quality in the common carp,

Cyprinus carpio, and turbot, *Psetta maxima*, were lower during the early and late spawning season (Christ et al. 1996; Suquet et al. 1998). Similarly, sperm quality decreased over the reproductive season for Atlantic halibut, *Hippoglossus hippoglossus*, Atlantic cod, *Gadus morhua*, and sole, *Solea senegalensis*, (Methven and Crim 199; Rouxel et al. 2008; Beirao et al. 2011). While there are fewer seasonal studies on sperm quality in invertebrates, the overarching trends remain evident. Greenlip abalone (*Haliotis laevigata*) sperm had higher motility and fertilization capacity during the middle of the reproductive season than the beginning or the end of the season (Liu et al. 2015). Thus, sperm analysis can be used to determine the optimal period in which sperm should be collected. However, seasonal variation in sperm biological parameters of freshwater mussel species are lacking in the scientific literature.

In the present study, our goal was to monitor sperm production and morphology parameters of two long-term brooding freshwater mussel species, *L. subrostrata* and *L. straminea* (Williams et al. 2008) over their spawning season. These two species were ideal for this study, because both display sexual dimorphism. *L. subrostrata* females exhibit an obliquely truncated posterior end, while in males, the posterior end is bluntly pointed (Williams et al. 2008). In *L. straminea*, females express a greater inflation and more rounded posterior end, whereas males were less inflated and exhibited a straighter posterior region (Williams et al. 2008). These shell features allowed for easy identification of males and females. Additionally, both species frequently inhabit stream pools and reaches with little current (Williams et al. 2008), allowing for natural reproduction in ponds at Auburn University.

The objectives of this study were to follow temporal changes in sperm concentration and morphology, identify and measure intraspecific heterogeneity for sperm morphometry traits, and develop an efficient method to quantify sperm concentration using a microspectrophotometer

(NanoDrop®). Monitoring a spawning profile for two long-term brooding species will provide novel information on freshwater mussel reproduction and gamete biology. Additionally, the regressions based on absorbance can be utilized as a non-lethal method to rapidly quantify sperm density for vulnerable species. These results can be used to further understand sperm quality, fertilization dynamics, and future cryopreservation conditions for freshwater mussels.

2.2 Materials and Methods

2.2.1 Animal collection and husbandry

Two long-term brooding species, *L. subrostrata* and *L. straminea*, were used for the following experiments. Males were collected on 13 June 2018 from ponds at South Auburn Fisheries Research Station, Auburn University. *L. subrostrata* (n = 180) and *L. straminea* (n = 105) were collected, tagged with hall print tags, and measured (length, width, and height). Both species were held separately in two ponds (one pond per species). Within each pond, 15 mesh cages approximately 1' in diameter were distributed along the full length of the pond and held in place with plastic stakes. *L. subrostrata* and *L. straminea* were distributed evenly into the cages with n = 12 and n = 7 mussels per cage, respectively. Males were placed in cages with their posterior end down into the sediment. A HOBO temperature logger (HOBO Pendant® MX Temperature/Light Data Logger, Onset, USA) was placed underwater and just above the pond sediment to track temporal changes in temperature within each pond.

For experiments, mussels were placed on wet paper towels in a Styrofoam cooler and transported to the Auburn University Reproductive Physiology Laboratory in the E.W. Shell

Fisheries Center, Auburn, Alabama (32° 40' 1.5" N, 85° 29' 22.1" W). Before gamete analysis, morphometrics including length (± 0.01 mm), width (± 0.01 mm), height (± 0.01 mm), and weight (± 0.01 g) were taken for each male (Table 2.1).

2.2.2 Experiment 1: Temporal variations in sperm concentration and head morphology

Sampling males

L. subrostrata (n = 30) and *L. straminea* (n = 30) males were sampled throughout the spawning season to follow their sperm concentration and morphology. The sampling start date for the temporal study was determined by the presence of mature sperm in the gonad. Additionally, female gills (n = 5) of both species were observed during sampling to detect the brooding of glochidia, and gravid females were observed by 24 October. Thus, the temporal variation timeline coincided with both spawning seasons. Ponds were sampled every two weeks on the dates of 29 August, 13 September, 26 September, 10 October, 24 October, 7 November, and 20 November 2018.

At each sampling time, 5 cages were randomly chosen without replacement from 15 cages within each pond. One male was randomly selected from each cage to get a total of 5 males. Mussels were opened by cutting the adductor muscles with a scalpel. For each male, three samples of testicular fluid, including sperm, were collected from the center of the gonad and half a centimeter on either side (Fig. 2.1). Sperm collection was conducted using a small pipette tip to draw a 1 µL sample directly from the gonad.

Determination of sperm concentration using a hemocytometer

Sperm concentration, sperm/mL, was determined for each male using a Neubauer hemocytometer. Once sperm were diluted in 1X PBS, samples were homogenized for ~10 s, then 10 µL was pipetted onto the hemocytometer. Sperm randomly settled onto a 5 × 5 grid (1 mm^2), where sperm inside of five squares (0.2 mm^2) (top left, top right, bottom right, bottom left, and center) were counted. To get the average cell density of the diluted sperm in the 5 × 5 grid, the five squares were averaged and multiplied by 5 to estimate sperm cells in the entire 5 × 5 grid. The distance from the floor of the chamber to the glass coverslip is 0.1 mm. The total volume of the counting area is 10^{-4} cm^3. The dilution factor of the semen to seawater ratio was calculated. The dilution factor was multiplied by the sperm density in the 5 × 5 grid and multiplied by 10^4 to determine the sperm density of the testicular fluid for each male. Sperm concentrations from the samples of the three collection points, left, center, and right of the gonad (Fig. 2.1), from each male were averaged.

Determination of sperm head morphology using scanning electron microscopy

To better understand temporal changes in sperm morphology, sperm were sampled during early (26 September), middle (24 October), and late (20 Nov) portions of the 2018 temporal variation study. Sperm used in this study were from a subset of males (5 males × 2 species × 3

sampling times = 30) that were sampled for sperm concentration. All chemicals were of reagent grade (Electron Microscopy Sciences, Fort Washington, PA). Sperm collected from each male were fixed in 2.5% glutaraldehyde in 0.1 M cacodylate buffer (pH 7.5) at a ratio of 1:100 (v:v) sperm to glutaraldehyde, respectively. Sperm dilutions were held at 4 °C until further processing.

In between every step, sperm samples were centrifuged at 14,000 RPM until a pellet formed in the bottom of the microcentrifuge tubes, and the supernatant was removed using a pipette. First, sperm samples were washed three times with approximately 0.5 mL of 0.1 M cacodylate buffer for 15 min. Samples were then post-fixed for 1 h with 1% osmium tetroxide (OsO_4), just enough to barely cover the samples, at room temperature and in the dark. Then, samples were washed with 0.1 M cacodylate buffer for 10 min. Samples were dehydrated through a series of 30, 50, 70, 80, 90, and 95% ethanol (EtOH) for 15 min each and 100% EtOH two times for 15 min each. Glass coverslips were broken into small pieces and attached to an aluminum stub with carbon tape. Ethanol-hexamethydisilazane (HMDS) was added to all samples, mixed, and a small drop was pipetted onto the glass coverslip to dry completely. Samples were then sputter coated with gold using an EMS 550X Auto Sputter Coating Device (Electron Microscopy Science, Hatfield, PA). Micrographs of sperm were taken using Zeiss EVO 50 Variable Pressure Scanning Electron Microscope (Carl Zeiss Microscopy, LLC, White Plains, NY) at magnification of 4000× (Fig. 2.2AB).

Sperm morphology including sperm head length, width, and area were measured using ImageJ software. ImageJ is an open source JAVA application (National Institutes of Health, Bethesda, MD, USA) and is available for download at http://rsbweb.nih.gov/ij/. First, ImageJ (OS X 10.7 or later) was opened and the digital image of a SEM micrograph was loaded (click File » Open » find the image). Next, the Straight-Line selection tool, located on the toolbar, was

used to make a straight line on the 10 µm scalebar located on the SEM micrograph. The Set Scale dialog was then opened (click Analyze » Set Scale), and 10 was entered into the Known Distance box and µm was entered into the Unit of Length box. ImageJ then automatically filled in the Distance in Pixels box based on the length of the straight line. For both species, 20 sperm heads were measured for each male. Length and width were measured using Straight Line tool and area was measured using the Freehand tool.

2.2.3 Experiment 2: Quantifying male-to-male variation in sperm morphology

L. subrostrata (n = 10) and *L. straminea* (n = 10) were sampled on 9 September 2019 and 2 October 2019, respectively, from ponds at the E.W. Shell Fisheries Center, Auburn University. *L. subrostrata* males were randomly selected from 4 floating cages in a pond. *L. straminea* were collected along the banks of a pond. Sperm (~20 µL) were collected from the gonad and stored in 1 mL Eppendorf tubes. Cells were then stained using Hemacolor (Merck standard kit, Darmstadt, Germany, Cat. No., 11661). In brief, 5 µL of sperm was added to 95 µL of sodium citrate (Remel, Lenexa, KS, USA) and gently shaken for 30 s to homogenize the solution. Next, 5 µL of the sperm solution was pipetted onto a microscope slide, prewashed with 95% ethyl alcohol, and the edge of a clean microscope slide was used to quickly smear the sperm solution across the microscope slide. Sperm smears then went into a fixative for 15 s, a red stain for 3 min, and were submersed in a blue stain (5 × 1 s dips) and then thoroughly rinsed in distilled water. Microscope slides were then placed vertically and allowed to air dry. Finally, smears were permanently sealed with Eukitt mounting medium (Kindler and Co., Freiburg, Germany) and topped with a coverslip. Photos were taken with a camera (Axiocam 202 mono, Carl Zeiss Meditec Inc., CA,

USA) attached to a microscope (Axio Imager.A2, Carl Zeiss Meditec Inc., CA, USA) at 100× magnification (Fig. 2.2C). Sperm morphology including sperm head length, width, flagella length, and total length (defined as head length + flagella length) were measured using ImageJ software, as above. For both species, each male had 45 sperm measured. For a sperm cell to be selected for measurement, the head and flagella could not overlap any other sperm, and the sperm cell could not have any deformities such as an exploded head or broken flagellum.

2.2.4 Experiment 3: Quantifying sperm concentration using a microspectrophotometer

L. subrostrata (n = 7) and *L. straminea* (n = 7) were randomly selected from 15 cages from each pond on 1 and 17 November 2018, respectively and sperm were collected, as above. 1 µL sperm from each male were diluted with 999 µL 1X PBS. Each sperm dilution was counted using a Neubauer hemocytometer to calculate sperm concentration (according to Section 2.2.2). Three replicates were counted for each sample and averaged to determine sperm concentration. Thereafter, seven different cell concentrations were made by diluting sperm with 1X PBS to get approximately 1×10^9, 8×10^8, 4×10^8, 2×10^8, 1×10^8, 8×10^7, 4×10^7 cells/mL for *L. subrostrata* and 6×10^8, 4×10^8, 2×10^8, 1×10^8, 8×10^7, 4×10^7, 2×10^7 cells/mL for *L. straminea*. Sperm concentration was then determined for each dilution using a hemocytometer.

A microspectrophotometer (NanoDrop 2000, Thermo Scientific, Wilmington, DE) set to ‘‘Cell Culture’’ module was used to obtain absorbance readings for the seven sperm dilutions from both mussel species. The microspectrophotometer was cleaned with distilled water and Kim-wipes before and at the end of the experiment so that the absorbance read 0.000. The buffer used for suspending the sperm, 1X PBS, was used as a reference blank before measuring the

samples. Sperm solutions were gently inverted 10 times to homogenize the sample before each reading, and a volume of 2 μL was pipetted onto the instrument. According to the manual, to ensure proper sample column formation between the upper and lower pedestals, 2 μL was used instead of 1 μL. Absorbances for sperm dilutions were measured three times at each wavelength (300, 600, and 700 nm) and averaged.

2.2.5 Statistical analyses

Data were analyzed using SAS statistical analysis software (v. 9.1; SAS Institute Inc., Cary, NC, USA). Residuals were tested for normality (Shapiro–Wilk test) and homogeneity of variance (plot of residuals vs. predicted values). Data were $\log_{10}$ transformed to meet assumptions of normality and homoscedasticity when necessary. Error bars represent least square means standard error. Treatment means were contrasted using the Tukey's test. Alpha was set at 0.05.

Temporal changes in sperm concentration and head morphology (i.e. sperm head length, width, and area) were analyzed using a series of repeated measures factorial ANOVA models. A series of one-way ANOVA models were also used to examine the degree of male-to-male variability between sperm morphological indices (i.e. sperm head length, width, flagella length, and total length). Correlation analyses (Pearson's correlation) were then used to measure the associations between the sperm morphological indices. Linear and polynomial regression analysis were used to examine the relationship between sperm concentration and absorbance by use of a microspectrophotometer. Separate regressions were run at each absorbance.

2.3 Results

2.3.1 Experiment 1: Temporal variations in sperm concentration and head morphology

For both freshwater mussel species, *L. subrostrata* and *L. straminea*, there was a temporal change in sperm concentration sampled from 29 August to 20 November 2018 (P <.0001) (Fig. 2.3 AC). *L. subrostrata* sperm concentration increased from 29 August to 26 September with cell densities of 1.12×10^9 to 19.60×10^9 cells/mL, respectively (Fig. 2.3A). Highest sperm concentrations were recorded from 26 September to 7 November, thereafter the concentration of sperm in the reproductive organ significantly declined (Fig. 2.3A). During the sampling period, temperature in the *L. subrostrata* pond declined from ~30.5 ºC to 11.5 ºC from 29 August to 20 November, respectively (Fig. 2.3B). *L. straminea* sperm concentration significantly increased from 29 August to 13 September where it peaked at 20.02×10^9 cells/mL (Fig. 2.3C). Sperm density was highest from 13 September to 26 September and declined thereafter (Fig. 2.3C). Pond temperature in the *L. straminea* pond declined from ~31.2 ºC to ~11.0 ºC from 29 August to 20 November, respectively (Fig. 2.3D).

Over time, both freshwater mussel species exhibited a significant (all $P \leq 0.007$) increase in sperm morphology parameters including width, length, and area of the sperm head (Table 2.2). During the middle portion of the seasonal study, *L. subrostrata* sperm measured 1.61 ± 0.01, 3.38 ± 0.04, and 4.52 ± 0.08 for width, length, and area, respectively. For *L. subrostrata*, width and length increased from early to late spawning season, and area significantly increased from early to middle to late spawning season (Table 2.2). Similarly, *L. straminea* sperm measured

1.61 ± 0.01, 3.37 ± 0.04, and 4.52 ± 0.07 during the middle of spawning season for width, length, and area, respectively. For *L. straminea*, width significantly increased from early to middle to late spawning season, while length and area increased from early to late spawning season (Table 2.2).

2.3.2 Experiment 2: Quantifying male-to-male variation in sperm morphology

There was significant variation among individual males in total sperm head width and length between the males for *L. subrostrata* (Fig. 2.4AB; $P < 0.0001$) and also for *L. straminea* (Fig. 2.4EF; $P < 0.0001$). Moreover, *L. subrostrata* showed a high-degree of variability between males for flagella length ($P = 0.0013$, Fig. 2.4C) and total length ($P < 0.001$, Fig. 2.4D), while these sperm morphological traits did not vary for *L. straminea* ($P \leq 0.238$; Fig. 2.4GH). There were positive correlations between sperm head length and width for *L. subrostrata* ($P < 0.0001$, $r = 0.78$) and *L. straminea* ($P < 0.0001$, $r = 0.43$). All other correlations were non-significant.

2.3.3 Experiment 3: Quantifying sperm concentration using a microspectrophotometer

There were positive quadratic relationships between hemocytometer counts and absorbance for *L. subrostrata* at 300 ($P < 0.0001$, $R^2 = 0.96$, $y = -2.79\times10^8x + 4.69\times10^8x^2 + 8.62\times10^7$; Fig. 2.5A), 400 ($P < 0.0001$, $R^2 = 0.96$, $y = -3.38\times10^8x + 5.39\times10^8x^2 + 9.67\times10^7$), and 600 nm ($P < 0.0001$, $R^2 = 0.97$, $y = -3.80\times10^8x + 6.53\times10^8x^2 + 9.91\times10^7$). Similarly, positive quadratic relationships existed for *L. straminea* at 300 ($P < 0.0001$, $R^2 = 0.86$, $y = 5.82\times10^7x + 1.94\times10^8x^2 + 7.78\times10^6$, Fig. 2.5B), 400 ($P < 0.0001$, $R^2 = 0.85$, $y = -3.61\times10^7x + 2.69\times10^8x^2 +$

2.64×10^7), and 600 nm ($P < 0.0001$, $R^2 = 0.90$, $y = -8.60\times10^7x + 3.84\times10^8x^2 + 3.48\times10^7$). Linear relationship models were also generated at 300 nm (Fig. 2.5AB), where positive relationships were detected for both *L. subrostrata* ($P < 0.0001$, $R^2 = 0.85$, $y = 1.11\times10^9x - 9.34\times10^8$) and *L. straminea* ($P = 0.001$, $R^2 = 0.41$, $y = 6.01\times10^8x - 3.60\times10^8$).

2.4 Discussion

The present study describes seasonal variations in sperm concentration, morphology, and male-to-male variability in *L. subrostrata* and *L. straminea.* To the best of our knowledge, this is one of the first studies to describe seasonal changes in sperm production and morphology for unionid freshwater mussel species. The sperm concentration profile for *L. subrostrata* follows a bell-shaped function with peak sperm production from late September to early November, while the seasonal profile for *L. straminea* follows a bell-shaped function that is skewed and had highest sperm densities for a shorter period of time from early to late September. Overall, both species displayed an increase and subsequent decrease in sperm concentration during the fall season which is expected of long-term brooders (Williams et al. 2008). These profiles can be utilized to better understand freshwater mussel sperm biology and aid in conservation strategies for other long-term brooders. Additionally, as conservation efforts shift towards freshwater mussel propagation and cryopreservation tools, knowledge on the timing of peak sperm production is invaluable. The collection of high quantity and quality sperm is important for cryopreservation as post-thawed sperm usually decreases in quality (Paniagua-Chavez Tiersch 2001; Yang et al. 2012).

The ultrastructural analysis from SEM of freshwater mussel sperm revealed an increase in sperm head width, length, and area from 26 September to 20 November, for both species. These changes in sperm size could be due to sperm senescence and a decrease in sperm membrane viability. Similar to our results, sperm head length for *L. subrostrata* (3.38 μm) and *L. straminea* (3.37 μm) were close to the freshwater mussel *Margaritifera laevis* (3.2 μm) (Kobayashi et al. 2018) and *Truncilla truncata* (3.2 μm) (Waller and Lasee 1997). The mean total lengths of *L. subrostrata* (40.0 μm; Fig. 2.4D) and *L. straminea* (41.6 μm; Fig. 2.4H) sperm were similar to *M. laevis* sperm length which measured around 40 μm (Kobayashi et al. 2018).

Due to the diversity of some morphological features, ultrastructural analyses of sperm can provide insights into phylogenetic issues in bivalves (e.g., Healy, 1996; Healy et al. 2000, 2008; Kim et al. 2013). Comparing sperm ultrastructure can generate characters of taxonomic and phylogenetic significance (Gwo et al. 2002). Many studies utilize sperm morphology in evaluating molluscan phylogeny (Franzen, 1983; Healy, 1995a,b). Specifically, several investigations use sperm ultrastructure to distinguish closely related species (Hodgson et al. 1990; Walker et al. 1996).

The results on sperm concentration and morphology can be used to better understand sperm aging or senescence. As sperm ages, it undergoes biochemical and morphological changes, in which cell motility and fertilization capacity is functionally impaired (Reinhardt, 2007). Sperm activity kinetics, percent motility and velocity, can be indicators of sperm quality (Billard 1978; Stoss 1983; Lahnsteiner et al. 1996) which often changes over the seasonal spawning cycle.

The study on male-to-male variability in sperm morphology revealed significant variation in total sperm head width and length between the males for *L. subrostrata* and *L. straminea.*

Interestingly, the flagella length and total length of *L. subrostrata* had high variability among males, while *L. straminea* did not. Male-to-male variability is also documented in Pacific oysters, *Crassostrea gigas*, Eastern oyster, *C. virginica* (Dong 2005; Paniagua-Chavez and Tiersch, 2001), zebrafish, *Danio rerio*, (Harvey et al.1982), and rainbow trout, *Oncorhynchus mykiss,* (Stoss and Holtz 1983). This is important because sperm morphology traits are typically correlated to swimming speed (Tuset et al. 2008) and sperm motility. Furthermore, high sperm motility is essential for fertilization and highly correlated to fertilization success (Rurangwa et al. 2004).

Estimating sperm concentration using microspectrometery proved to be a reliable method for freshwater mussel sperm quantification. Quadratic regressions made at 300, 400, and 600 nm wavelengths produced R^2 values ≥ 0.85 for both species, while linear regressions at 300 nm produced R^2 values ≥ 0.41. For both freshwater mussel species, the quadratic regressions utilized a broader absorbance range from 0.0 to 2.0, and the linear regressions utilized the higher sperm concentrations and focused on a narrower range of absorbances from 0.8 to 1.8. These regressions can now be used to facilitate breeding of freshwater mussels. For instance, these equations provide a quick, objective way to estimate sperm concentration with less room for error than manually counting. Additionally, microspectrometery requires low sample volumes which may be limiting for small-bodied organisms or species of concern (Tan et al. 2010). This method also opens more research opportunities on sperm production and quality for freshwater mussels, especially when combined with non-lethal sperm collection techniques (Tan et al. 2010; Fritts et al. 2015).

2.5 Conclusions

Overall, our study found significant temporal changes in freshwater mussel sperm parameters which coincided with the spawning season for *L. subrostrata* and *L. straminea*. For both species, freshwater mussels sampled over this three-month study had significant changes in sperm concentration and morphology, which was highly variable among individual males of each species. This study corroborates previous literature on other species where sperm biomarkers (e.g. concentration) declined towards the end of the spawning season (Christ et al. 1996; Methven and Crim 1991; Suquet et al. 1998; Rouxel et al. 2008; Beirao et al. 2011). Additionally, our study effectively developed a method to quantify sperm concentration using microspectrophotometry. The regressions can accurately estimate sperm concentrations and serve as a model for the quantification of sperm for other freshwater mussel species. Ultimately, the results provide a baseline to further improve knowledge on sperm biology, fertilization dynamics, and cryopreservation conditions for imperiled freshwater mussel species.

Acknowledgements

This work was supported by the Alabama Agriculture Experimental Station & the USDA National Institute of Food & Agriculture, Hatch project (1013854).

References

Arey, L. B. 1932. The formation and structure of the glochidial cyst. Biological Bulletin 62:212-221.

Barnhart M. C., and A. Roberts. 1997. Reproduction and fish hosts of Unionids from the Ozark Uplifts. Pages 14-20 in KS Cummings el al. editors. Conservation and management of freshwater mussels II: Initiatives for the future. Upper Mississippi Conservation Committee, Rock Island, Illinois, USA.

Beirao, J., F. Soares, M. P. Herraez, M. T. Dinis, and E. Cabrita. 2011. Changes in *Solea senegalensis* sperm quality through the year. Animal Reproduction. Sci 126:122-129.

Benz, G. W. and D. E. Collins, (eds). 2004. Aquatic Fauna in Peril: The Southeastern Perspective. Southeast Aquatic Research Institute, Dectur, GA.

Billard, R. 1978. Changes in structure and fertilizing ability of marine and freshwater fish spermatozoa diluted in media of various salinities. Aquaculture 14:187-198.

Bishop, J. D., and A. J. Pemberton. 2006. The third way: spermcast mating in sessile marine invertebrates. Integrative and Comparative Biology 46:398-406.

Bogan, A. 1993. Freshwater Bivalve Extinctions (Mollusca, Unionida): A search for causes. American Zoologist 33(6):599-609.

Cabrita, E., V. Robles, and M. P. Herráez. 2009. Sperm quality assessment. In: Cabrita, E., V. Robles, and M. P. Herráez. (eds), Methods in Reproductive Aquaculture: Marine and Freshwater Species. Biology Series. CRC Press (Taylor and Francis Group), Boca Raton, Florida, USA, pp. 93-148.

Christ, S. A., G. P. Toth, H. W. McCarthy, J. A. Torsella, and M. K. Smith. 1996. Monthly

variation in sperm motility in common carp assessed using computer-assisted sperm analysis (CASA). Journal of Fish Biology 48:1210-1222.

Dong, Q. 2005. Comparative studies of sperm cryopreservation of diploid and tetraploid Pacific Oysters. Doctor of Philosophy Thesis. Agricultural and Mechanical College, Louisiana State University.

Downing, J. A., P. Van Meter, and D. A. Woolnough. 2010. Suspects and evidence: a review of the causes of extirpation and decline in freshwater mussels. Animal Biodiversity and Conservation 33:151-185.

Eckelbarger, K. J., and C. V. Davis. 1996. Ultrastructure of the gonad and gametogenesis in the eastern oyster, *Crassostrea virginica*. II. Testis and spermatogenesis. Marine Biology 127:89-96.

Erkan, M., and M. Sousa. 2002. Fine structural study of the spermatogenic cycle in *Pitar rudis* and *Chamelea gallina* (Mollusca, Bivalvia, Veneridae). Tissue and Cell 34:262-272.

Franzen, A., 1983. Ultrastructural studies of spermatozoa in three bivalve species with notes on evolution of elongated sperm nucleus in primitive spermatozoa. Gamete Research 7:199-214.

Fritts, A. K., J. T. Peterson, J. M. Wisniewski, and R. B. Bringolf. 2015. Nonlethal assessment of freshwater mussel physiological response to changes in environmental factors. Canadian Journal of Fisheries and Aquatic Sciences 72(10):1460-1468.

Gough, H. M., A. M. Gascho Landis, and J. A. Stoeckel. 2012. Behavior and physiology are linked in the responses of freshwater mussels to drought. Freshwater Biology 57:2356-2366.

Graf, D.L. and K. S. Cummings. 2007. Review of the systematics and global diversity of

freshwater mussel species (Bivalvia: Unionoida). Journal of Molluscan Studies 73:291-314.

Gwo, J. C., W. T. Yang, Y. T. Sheu, and H. Y. Cheng. 2002. Spermatozoan morphology of four species of bivalve (Heterodonta, Veneridae) from Taiwan. Tissue and Cell 34(1):39-43.

Haag, W. R. and M. L. Warren. 1997. Host fishes and reproductive biology of 6 freshwater mussel species from the Mobile Basin, USA. Journal of the North American Benthological Society 16:576-585.

Haag, W. R. and M. L. Warren. 2008. Effects of severe drought on freshwater mussel assemblages. Transactions of the American Fisheries Society 137:1165-1178.

Haag, W. R., and J. D. Williams. 2014. Biodiversity on the brink: An assessment of conservation strategies for North American freshwater mussels. Hydrobiologia 735(1):45-60.

Harvey, B., R. N. Kelley, and M. J. Ashwood-Smith. 1982. Cryopreservation of zebrafish spermatozoa using methanol. Canadian Journal of Zoology 60:1867-1870.

Healy, J. M. 1995a. Comparative spermatozoal ultrastructure and its taxonomic and phylogenetic significance in the bivalve order Veneroida. In: Jameison, B. G. M., J. Ausio, and J. Justine, (eds) Advances in Spermatozoal Phylogeny and Taxonomy. Mem. Mus. Natn. Hist. Nat, Paris 166:155-166.

Healy, J. M. 1995b. Sperm ultrastructure in the marine bivalve families Carditidae, and Crassatellidae and its bearing on unification of the Crassatelloidea with the Carditoidea. Zoologica Scripta, 24, 21-28.

Healy, J. M., 1996. Molluscan sperm ultrastructure: correlation with taxonomic units within the Gastropoda, Cephalopoda and Bivalvia. In: Taylor, J. (ed), Origin and Evolutionary Radiation of the Mollusca. Oxford University Press, pp. 99-113.

Healy, J. M., M. P. Mikkelsen, and R. Bieler. 2008. Sperm ultrastructure in *Hemidonax pictus* (Hemidonacidae, Bivalvia, Mollusca): comparison with other heterodonts, especially Cardiidae, Donacidae and Crassatelloidea. Zoological Journal of the Linnean Society 153:325-347.

Hodgson, A. N., and R. T. F. Bernard. 1986. Ultrastructure of the sperm and spermatogenesis of three species of Mytilidae (Mollusca, Bivalvia). Gamete Research. 15:123-135.

Hodgson, A. N., R. T. F. Bernard, and G. ven der Horst. 1990. Comparative spermatology of three species of Donax (Bivalvia) from South Africa. Journal of Molluscan Studies 56:257-265.

Ishibashi, R., A. Komaru, and T. Kondo. 2000. Sperm Sphere in Unionid Mussels (Bivalvia: Unionidae). Zoological Science 17(7):947-950.

Kat, P. W. 1984. Parasitism in the Unionacea (Bivalvia). Biological Reviews 59:189-207.

Karl, T. R., J. M. Melillo, T. C. Peterson, and S. J. Hassol, editors. 2009. Global Climate Change Impacts in the United States. Cambridge University Press.

Kobayashi, O., S. Tomizuka, S. Shimizu, and R. Machida. 2018. Spermatogenesis of the freshwater pearl mussel *Margaritifera laevis* (Bivalvia: Margaritiferidae): A histological and ultrastructural study. Tissue and Cell 55:39-45.

Lahnsteiner, F., B. Berger, T. Weismann, and R. A. Patzner. 1996. Motility of spermatozoa of *Alburnus alburnus* (Cyprinidae) and its relationship to seminal plasma composition and sperm metabolism. Fish Physiology and Biochemistry 15:167-179.

Layzer, J. B., M. E. Gordon, and R. M. Anderson. 1993. Mussels - the forgotten fauna of regulated rivers - a case-study of the Caney Fork River. Regulated Rivers: Research and Management 8:63-71.

Lynn, J. W. 1994. The ultrastructure of the sperm and motile spermatozeugmata released from the freshwater mussel *Anodonta grandis* (Mollusca, Bivalvia, Unionidae). Canadian Journal of Zoology 72:1452-1461.

Mackie, G. L. 1984. Bivalves. In: Tompa, A.S. N. H. Verdonk and J. A. M. van den Biggelaar, (eds). The Mollusca. Academic Press, Orlando, FL, USA. Pp. 351-418

Matteson, M. R. 1948. Life history of *Elliptio complanatus* (Dillwyn, 1817). The American Midland Naturalist 40(3):690-723.

McMahon, R. F. and A. E. Bogan. 2001. Mollusca: Bivalvia. In: Thorp, J. H. and A. P. Covich, (eds). Ecology and classification of North American freshwater invertebrates. Academic Press, San Diego. pp. 331-429.

Methven, D. A., and L.W. Crim. 1991. Seasonal changes in spermatocrit, plasma sex steroids, and motility of sperm from Atlantic halibut, *Hippoglossus hippoglossus*. In: Scott, A. P., J. P. Sumpter, D.E. Kime, and M. S. Rolfe, (eds), Proceedings of the Fourth International Symposium on the Reproductive Physiology of Fish. Published by Fish Symposium 91, Sheffield, U.K., p. 170.

O'Brien, C. A. and J. Brim-Box. 1999. Reproductive biology and juvenile recruitment of the shinyrayed pocketbook, *Lampsilis subangulata* (Bivalvia: Unionidae) in the Gulf Coast Plain. The American Midland Naturalist 142:129-140.

Paniagua-Chavez, C. G. and T. R. Tiersch. 2001. Laboratory studies of cryopreservation of sperm and trochophore larvae of the eastern oyster. Cryobiology 43:211-223.

Popham, J. D. 1979. Comparative spermatozoon morphology and bivalve phylogeny. Malacology Review. 12:1-20.

Reinhardt, K. 2007. Evolutionary consequences of sperm cell aging. Quarterly Reviews Biology

82:375-393.

Ram, J. L., P. P. Fong, and D. W. Garton. 1996. Physiological aspects of zebra mussel reproduction: maturation, spawning, and fertilization. American Zoologist 36:326-338.

Rouxel, C., M. Suquet, J. Cosson, A. Severe, L. Quemener, and C. Fauvel. 2008. Changes in Atlantic cod (*Gadus morhua* L.) sperm quality during the spawning season. Aquatic Research 39:434-440.

Rurangwa, E., D. E. Kime, F. Ollevier, and J. P. Nash. 2004. The measurement of sperm motility and factors affecting sperm quality in cultured fish. Aquaculture 234(1-4):1-28.

Stoss, J. 1983. Fish gamete preservation and spermatozoan physiology. Fish Physiology 9:305-350.

Stoss, J. and W. Holtz. 1983. Cryopreservation of rainbow trout (*Salmo gairdneri*) sperm III. Effect of proteins in the diluent, sperm from different males and interval between sperm collection and freezing. Aquaculture 31:275-282.

Suquet, M., C. Dreanno, G. Dorange, Y. Normant, L Quemener, J. L. Gaignon, and R. Billard. 1998. The ageing phenomenon of turbot spermatozoa: effects on morphology, motility and concentration, intracellular ATP content, fertilisation, and storage capacities. Journal of Fish Biology 52:31-41.

Tan, E., H. Yang, and T. R. Tiersch. 2010. Determination of sperm concentration for small-bodied biomedical model fishes by use of microspectrophotometry. Zebrafish 7(2):233-240.

Tuset, V. M., E. A. Trippel, and J. de Montserrat. 2008: Sperm morphology and its influence on swimming speed in Atlantic cod. J. Applied Ichthyology 24:4.

Vaughn, C. C. 2017. Ecosystem services provided by freshwater mussels. Hydrobiologia

810(1):15-27.

Vaughn, C. C. and C. C. Hakenkamp, 2001. The functional role of burrowing bivalves in freshwater ecosystems. Freshwater Biology 46:1431-1446.

Vaughn, C. C., S. J. Nichols and D. E. Spooner. 2008. Community and foodweb ecology of freshwater mussels. Journal of the North American Benthological Society 27: 41-55.

Vaughn, C. C. and C. M. Taylor. 1999. Impoundments and the decline of freshwater mussels: A case study of an extinction gradient. Conservation Biology 13:912-920.

Walker, G. K., M. G. Black, and C. A. Edwards. 1996. Comparative morphology of zebra (*Dreissena polymorpha*) and guagga (*Dreissena bugensis*) mussel sperm:light and electron microscopy. Canadian Journal of Zoology 74:809-815.

Waller D. L. and B. A. Lasee. 1997. External morphology of spermatozoa and spermatozeugmata of the freshwater mussel *Truncilla truncata* (Mollusca: Bivalvia: Unionidae). The American Midland Naturalist 138:220-223.

Watters G. T. and S. H. O'Dee. 1998. Metamorphosis of freshwater mussels glochidia (Bivalvia: Unionidae) on amphibians and exotic fishes. The American Midland Naturalist 139:49-57.

Watters, G. T., and S. H. O'Dee. 1999. Glochidia of the freshwater mussel Lampsilis overwintering on fish hosts. Journal of Molluscan Studies 65:453-459.

Williams, J. D., A. E. Bogan, and J. T. Garner. 2008. Freshwater mussels of Alabama and the Mobile Basin in Georgia, Mississippi, and Tennessee. University of Alabama Press, Tuscaloosa.

Williams, J. D., M. L. Warren, K. S. Cummings, J. L. Harris, and R. J. Neves. 1993.

Conservation status of freshwater mussels of the United States and Canada. Fisheries 18:6-22.

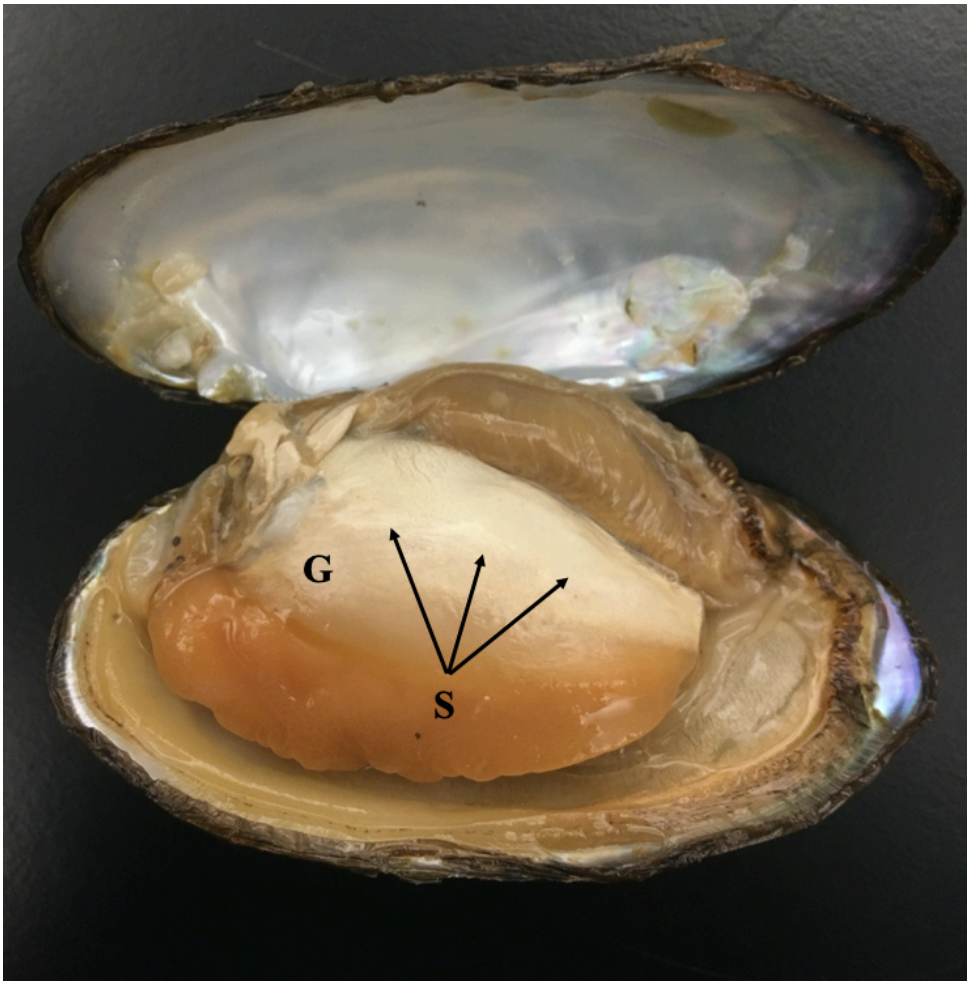

Figure 2.1 Sampling sperm from *Lampsilis straminea* where three samples of testicular fluid, including sperm, were collected from the center of the gonad and half a centimeter on either side. Sperm collection (S) was conducted using a small pipette tip to draw a sample directly from the gonad (G) designated by the black arrows.

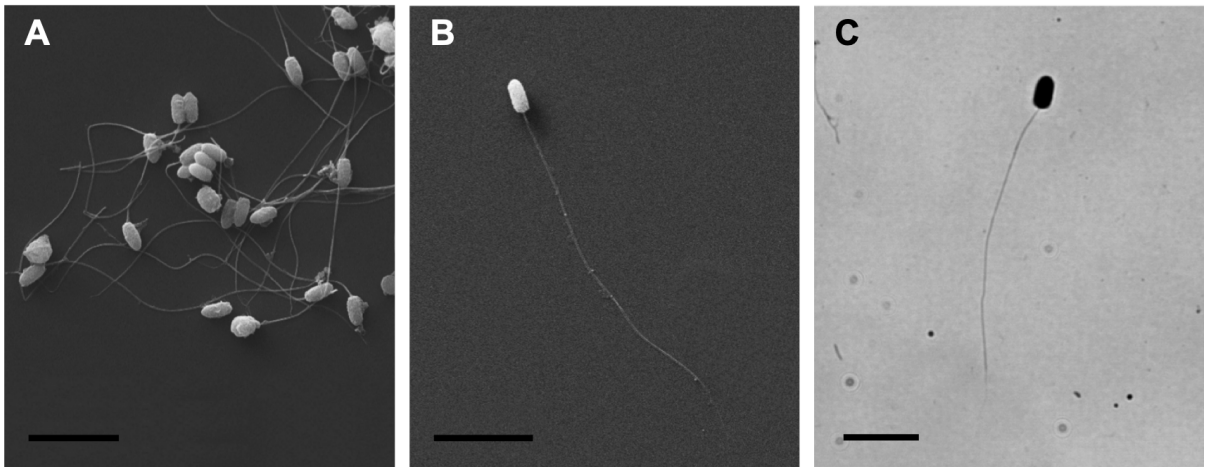

Figure 2.2 Ultrastructure of freshwater mussel sperm, *Ligumia subrostrata*, taken by SEM at a magnification of 4000 × (A) and 3790 × (B). *L. subrostrata* sperm fixed and stained with Hemacolor® taken at magnification of 100 × (C). Scale bars represent 10 μm for all photos.

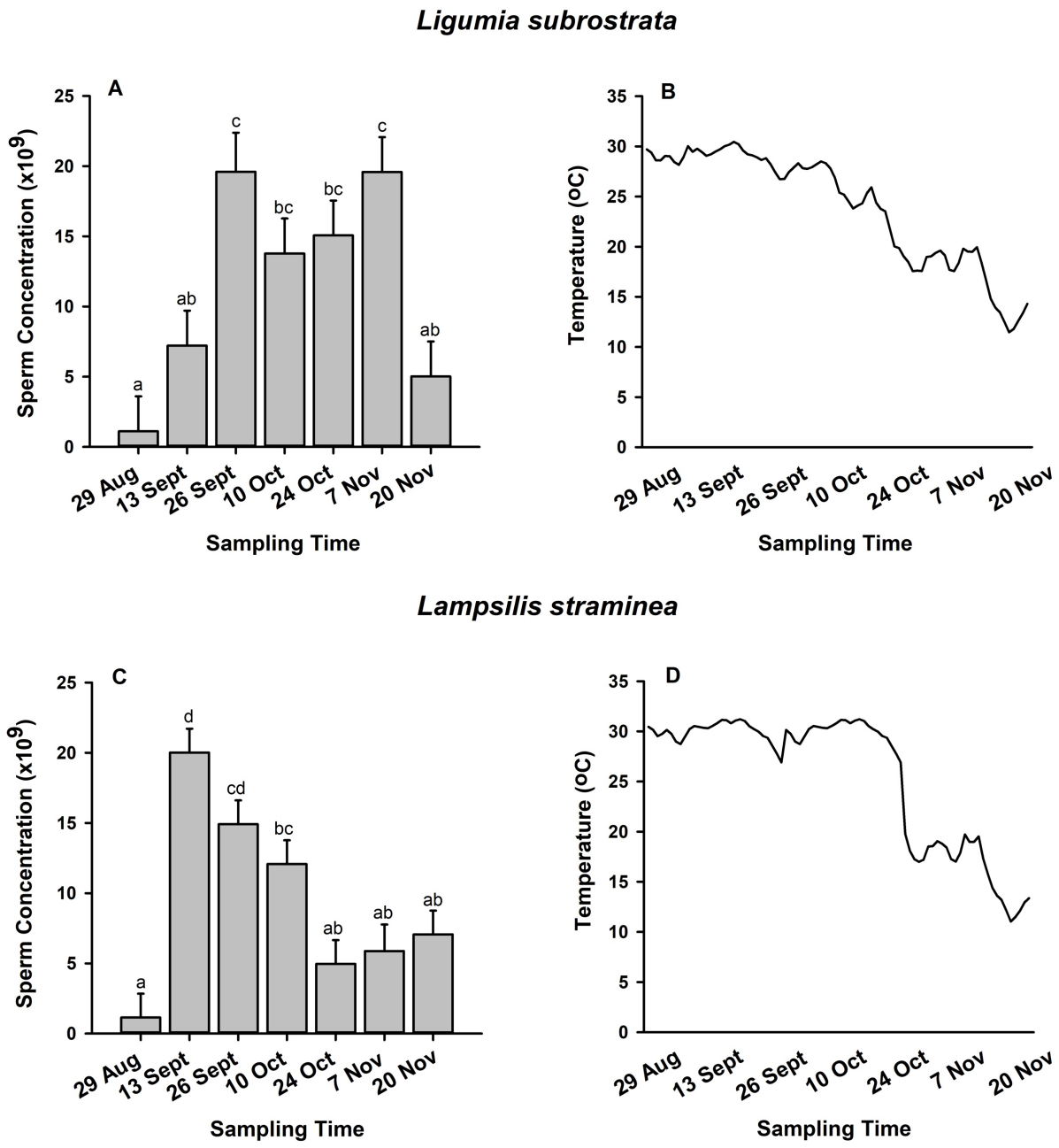

Figure 2.3 Temporal changes in sperm concentration (AC) and pond water temperatures (BD) for *Ligumia subrostrata* and *Lampsilis straminea* that were sampled from 29 August to 20 November 2018. Data were analyzed using a repeated measures factorial ANOVA model. Error bars represent least square means standard error. Treatments without a common superscript significantly differed ($P < 0.05$).

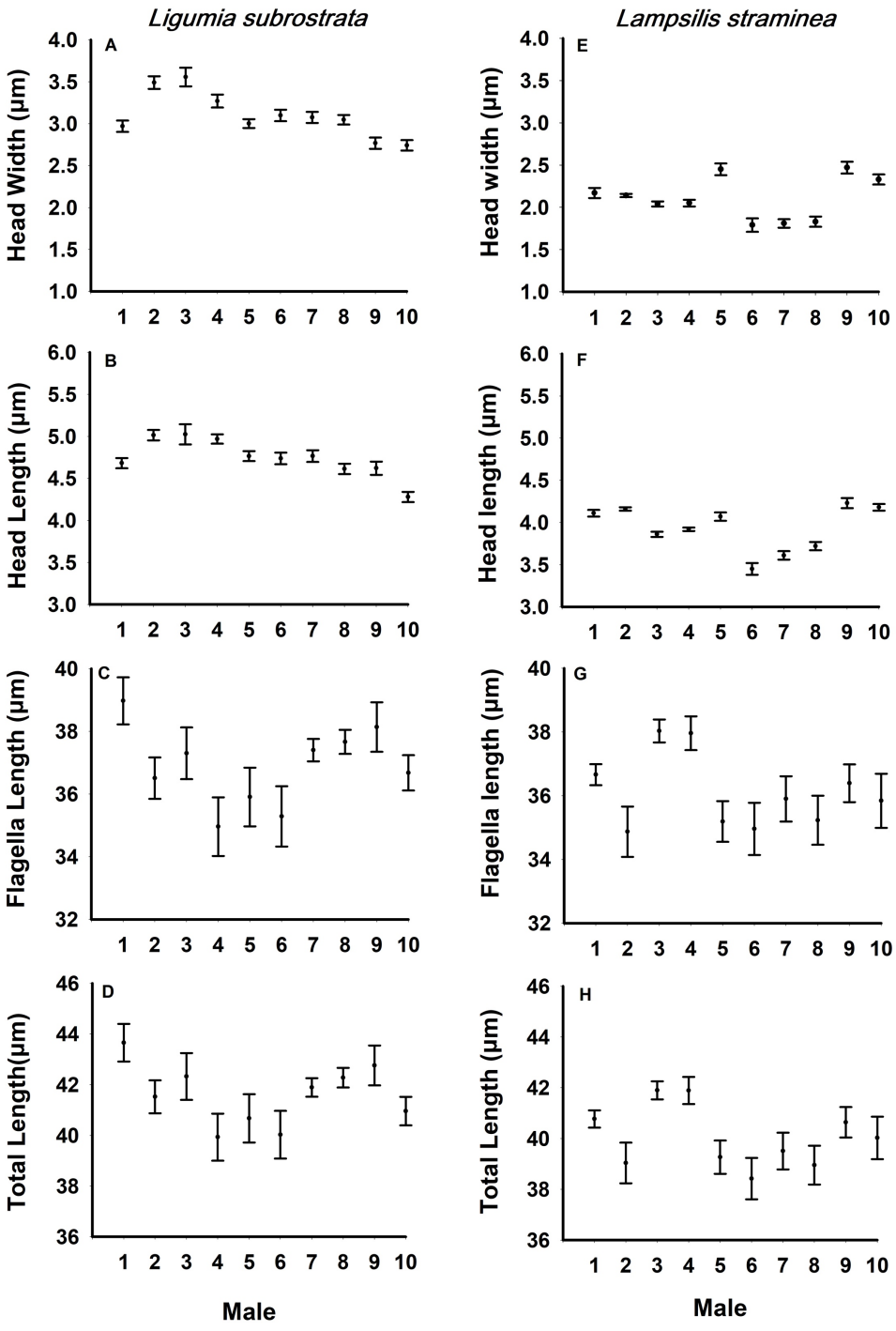

Figure 2.4 Variation within and among *Ligumia subrostrata* (n = 10) and *Lampsilis straminea* (n = 10) for total sperm head width (AE), head length (BF), flagella length (CG), and total length (DH). Mean ± SEM values per individual are represented. Male identification reflects arbitrary assignments.

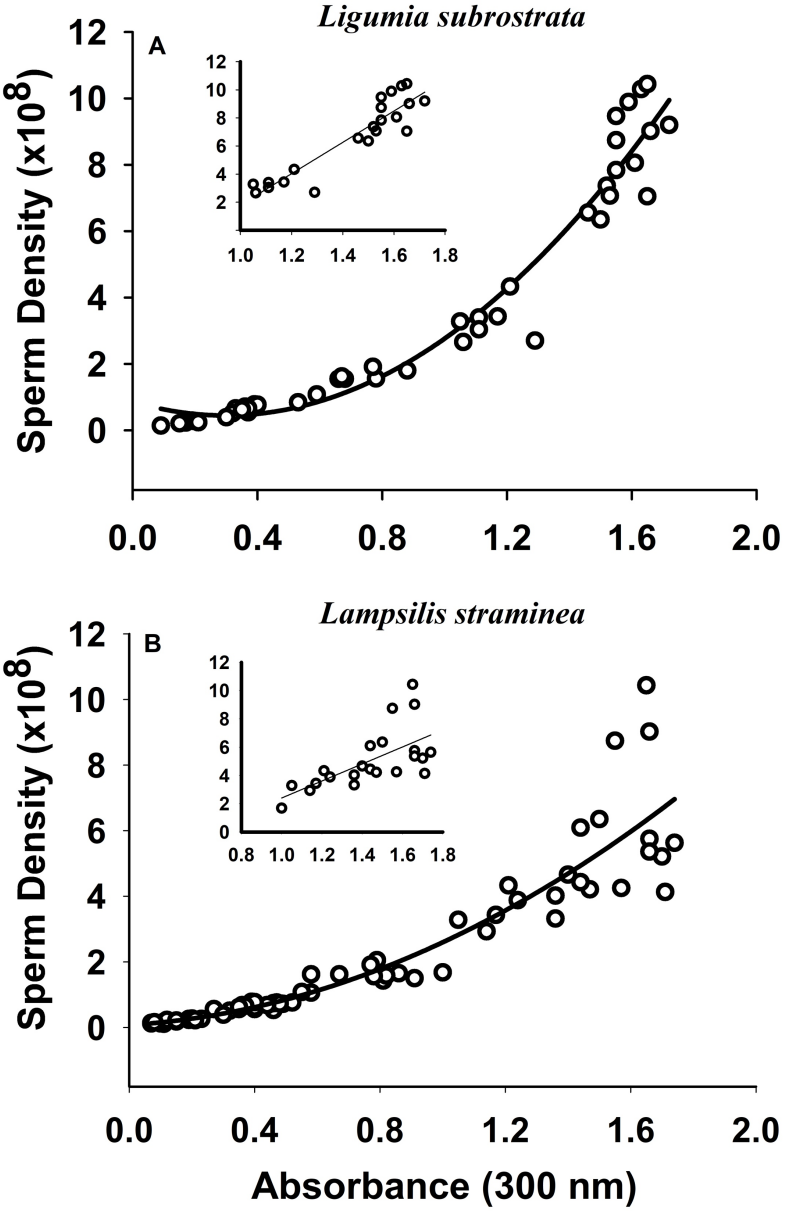

Figure 2.5 Regressions for two freshwater mussel species, *Ligumia subrostrata* (n = 7) (A) and *Lampsilis straminea* (n = 7) (B), that were used to relate sperm hemocytometer counts and absorbance via microspectrophotometery at 300 nm. For *L. subrostrata*, the positive quadratic regression and linear relationship resulted in $R^2 = 0.96$ and $R^2 = 0.85$, respectively. Whereas for *L. straminea,* positive quadratic regression and linear relationship generated a $R^2 = 0.86$ and $R^2 = 0.41$, respectively.

Table 2.1 Morphometrics including length (mm), width (mm), height (mm) and weight (g) of freshwater mussel species, *Ligumia subrostrata* (n = 5) and *Lampsilis straminea* (n = 5) used to study temporal variations in sperm concentration and head morphology.

Species	Date	Length ± SEM (mm)	Width ± SEM (mm)	Height ± SEM (mm)	Weight ± SEM (g)
L. subrostrata	29 Aug	75.78 ± 2.94	22.98 ± 1.10	35.76 ± 1.58	33.52 ± 3.78
	13 Sept	78.34 ± 3.55	24.42 ± 1.18	35.18 ± 2.15	29.01 ± 3.71
	26 Sept	77.18 ± 2.95	23.22 ± 1.26	29.16 ± 6.57	34.37 ± 1.18
	10 Oct	74.38 ± 3.03	34.12 ± 0.94	32.08 ± 3.35	32.08 ± 1.16
	24 Oct	72.86 ± 5.20	33.66 ± 1.97	44.48 ± 9.63	13.52 ± 2.76
	7 Nov	80.64 ± 2.97	36.66 ± 1.15	39.69 ± 4.57	13.22 ± 1.44
	20 Nov	76.82 ± 3.02	36.10 ± 1.51	34.57 ± 3.40	11.44 ± 0.85
L. straminea	29 Aug	68.56 ± 1.61	30.54 ± 2.13	41.68 ± 1.01	52.2 ± 4.03
	13 Sept	64.8 ± 1.45	28.64 ± 0.31	40.66 ± 1.45	40.58 ± 2.45
	26 Sept	69.42 ± 2.89	30.58 ± 0.53	42.38 ± 0.55	60.52 ± 4.98
	10 Oct	72.84 ± 4.63	31.18 ± 1.82	45.64 ± 2.27	66.03 ± 10.15
	24 Oct	67.96 ± 1.15	29.12 ± 0.6	41.86 ± 0.4	54.79 ± 2.08
	7 Nov	67.58 ± 4.29	27.76 ± 1.2	42.6 ± 2.16	51.88 ± 8.12
	20 Nov	66.78 ± 1.95	27.42 ± 0.82	39.86 ± 0.93	45.63 ± 2.69

Table 2.2 Temporal variation in sperm morphology for *Lampsilis straminea* (n = 5 at three sampling points) and *Ligumia subrostrata* (n = 5 at three sampling points). Micrographs were taken using SEM at a maginfication of 4000×, and 20 sperm heads per male were measured (width, length, and area) for both species. Data were analyzed using repeated measures factorial ANOVA models. Error bars represent least square means standard error. Treatments without a common superscript significantly differed ($P < 0.05$).

Species	Date	Width ± SEM (µm)	Length ± SEM (µm)	Area ± SEM (µm)
L. subrostrata	26 Sept	1.58 ± 0.01 a	3.27 ± 0.04 a	4.25 ± 0.08 a
	24 Nov	1.61 ± 0.01 ab	3.38 ± 0.04 ab	4.52 ± 0.08 b
	20 Nov	1.62 ± 0.01 b	3.44 ± 0.04 b	4.72 ± 0.08 c
L. straminea	26 Sep	1.57 ± 0.01 a	3.25 ± 0.04 a	4.30 ± 0.07 a
	24 Nov	1.61 ± 0.01 b	3.37 ± 0.04 ab	4.52 ± 0.07 ab
	20 Nov	1.67 ± 0.01 c	3.44 ± 0.04 b	4.69 ± 0.07 b